A COMPARATIVE ANALYSIS OF SINGE-STATE-TO-ORBIT ROCKET AND AIR-BREATHING VEHICLES

THESIS

Benjamin S. Orloff, Ensign, USN

AFIT/GAE/ENY/06-J13

DEPARTMENT OF THE AIR FORCE
AIR UNIVERSITY

AIR FORCE INSTITUTE OF TECHNOLOGY

Wright-Patterson Air Force Base, Ohio

The views expressed in this thesis are those of the author and do not reflect the official policy or position of the United States Air Force, the United States Navy, Department of Defense, or the U.S. Government.

AFIT/GAE/ENY/06-J13

A COMPARATIVE ANALYSIS OF SINGE-STATE-TO-ORBIT ROCKET AND AIR-BREATHING VEHICLES

THESIS

Presented to the Faculty

Department of Aeronautics and Astronautics

Graduate School of Engineering and Management

Air Force Institute of Technology

Air University

Air Education and Training Command

In Partial Fulfillment of the Requirements for the

Degree of Master of Science in Aeronautical Engineering

Benjamin S. Orloff, BS

Ensign, USN

June 2006

AFIT/GAE/ENY/06-J13

A COMPARATIVE ANALYSIS OF SINGE-STATE-TO-ORBIT ROCKET AND AIR-BREATHING VEHICLES

Benjamin S. Orloff, BS

Ensign, USN

Approved:

_____	_____
Milton E. Franke (Chairman)	Date
_____	_____
Ralph A. Anthenien (Member)	Date
_____	_____
Paul I. King (Member)	Date

Abstract

This study compares and contrasts the performance of a variety of rocket and airbreathing, single-stage-to-orbit, reusable launch vehicles. Fuels considered include bi-propellant and tri-propellant combinations of hydrogen and hydrocarbon fuels. Astrox Corporation's HySIDE code was used to model the vehicles and predict their characteristics and performance. Vehicle empty mass, wetted area and growth rates were used as figures of merit to predict the total cost trends of a vehicle system as well as the system's practicality. Results were compared to those of two-stage-to-orbit reusable launch systems using similar modeling methods. The study found that single-stage-to-orbit vehicles using scramjet airbreathing propulsion outperform rocket systems. Findings also demonstrate the benefits of using hydrocarbon fuel in the early phases of ascent to reduce the size and mass of launch vehicles. An all-hydrocarbon, airbreathing, single-stage-to-orbit vehicle was found to be a viable launch vehicle configuration and performed comparably to two-stage-to-orbit rocket systems.

To my fiancée

Acknowledgments

I would like to express my sincere appreciation to my thesis advisor, Dr. Milton Franke, for his support and guidance through the course of this research effort. I would also like to thank Capt. Joseph Hank who, as a master's student, mentored me and indoctrinated me to this material. I am very thankful to the Astrox Corporation, particularly Dr. Ajay Kothari, for all the assistance in understanding the tools and methods that enabled this study. My thanks also go to Dr. John Livingston who was always available for questions about the field of space access. His experience, insight and feedback were invaluable to his research effort.

I would like to thank my high school physics teacher, Tom Haff, for imbuing me with the intellectual curiosity to ask the questions and the analytical abilities to answer them. His love of science and space inspired within me the passion to explore.

I am indebted to my friends and co-workers who, through their humor and shenanigans, have made this educational experience both enlightening and entertaining.

Lastly, I would like to thank my family who has supported me throughout my education. Their love, confidence and compassion have enabled me to achieve my goals and given me the strength to persevere. Any success in life I may achieve will always be rooted in their support.

Benjamin S. Orloff

Table of Contents

Page

Page

Page

List of Figures

List of Tables

List of Symbols and Acronyms

Acronym	Description
AFB	Air Force Base
AFIT	Air Force Institute of Technology
ASC	Aeronautical Systems Center
ATO	Abort-to-Orbit
CEV	Crew Exploration Vehicle
CLV	Crew Launch Vehicle
DARPA	Defense Advanced Research Project Agency
DMSJ	Dual-Mode Scramjet
DOD	Department of Defense
ET	External Tank
GPS	Global Position System
GTOM	Gross Takeoff Mass
GTOW	Gross Takeoff Weight
GUI	Graphical User Interface
H	Hydrogen
HADO	Hypersonic Airbreathing Design Optimization
HC	Hydrocarbon
HTHL	Horizontal-Takeoff, Horizontal-Landing
HySIDE	Hypersonic System Integrated Environment
HySTP	Hypersonic Systems Technology Program
HyTech	Hypersonic Technology Program
I/O	Input / Output
ISS	International Space Station
KCS	Kennedy Space Center
LEO	Low-Earth Orbit
LH_2	Liquid Hydrogen
LOX	Liquid Oxygen
MECO	Main Engine Cutoff
NASA	National Aeronautics and Space Administration

NASP	National Aerospace Plane
OMS	Orbital Maneuvering System
POST	Program to Simulate Trajectories
RBCC	Rocket-Based Combined Cycle
RCS	Reaction Control System
RDP	Radial Deviation Parameter
RLV	Reusable Launch Vehicle
RTLS	Return-to-Launch Site
SI	International System
SRB	Solid Rocket Booster
SSME	Space Shuttle Main Engine
SSTO	Single-Stage-to-Orbit
STS	Space Transportation System
SysEl	System Element
T/W	Thrust-to-Weight Ratio
TBCC	Turbine-Based Combined-Cycle
TPS	Thermal Protection System
TSTO	Two-Stage-to-Orbit
USAF	United States Air Force
VTHL	Vertical-Takeoff, Horizontal-Landing

Acronym	Description
A_{exit}	Nozzle Exit Area
AR	Nozzle Area Ratio
C_D	Coefficient of Drag
C_L	Coefficient of Lift
CG	Center of Gravity
CP	Center of Pressure
D	Drag
EI_{sp}	Effective Specific Impulse

f_{empty} ..... Empty Mass Fraction

$f_{payload}$ ..... Payload Mass Fraction

G_{losses} ..... *Gravity Losses*

g ..... Acceleration due to Gravity

I_{sp} ..... Specific Impulse

L ..... Lift

m ..... Mass

$\dot{m}$ ..... Mass Flow

P ..... Pressure

q ..... Dynamic Pressure

SFC ..... Specific Fuel Consumption

S_{ref} ..... Wing Reference Area

T ..... Thrust

V ..... Velocity

W ..... Weight

Δh ..... Change in Altitude

Δt ..... Change in Time

ρ ..... Density

A COMPARATIVE ANALYSIS OF SINGE-STATE-TO-ORBIT ROCKET AND AIR-BREATHING VEHICLES

1. Introduction

1.1 Motivation

During the near half-century since the dawn of the space age, the ability to launch into Earth orbit has allowed for unprecedented advancements in both civilian and military applications. Satellite constellations provide world-wide coverage for weather forecasting, global telecommunications, Global Positioning System (GPS) navigation and ground imagery. Since the 1950's, both the U. S. military and the National Aeronautics and Space Administration (NASA) have searched for means of accessing space that are routine, reliable, responsive and affordable. In this endeavor, the focus has been placed mainly on expendable and hybrid launch systems (like the Space Shuttle). These systems are expensive to produce and incur high rates of cost-per-launch. The inability of these systems to launch on short notice make them incapable of being used in missions that require a fast response time. In the 1970's, NASA proposed a solution to this problem: the Space Shuttle.

Marketed to be an almost completely reusable launch vehicle (RLV), the Space Shuttle was designed to reduce the cost of launching satellites. The reusable nature of the system was meant to allow for large launch rates with a short turn-around time between subsequent launches of the same vehicle. Sadly, the Space Shuttle system failed to meet these goals. Current costs for launch sit at over $10,000 per pound of payload [10]. The highest launch rate the Space Shuttle fleet ever reached was only 11 launches per year

[10]. The logistics needed to turn around a Space Shuttle are both expensive and time consuming. These design flaws in system cost and logistics have prevented the Space Shuttle from attaining its initial goals. NASA's new design for the Crew Exploration Vehicle (CEV) may even be considered a step backwards in reusability [33]. The crew capsule will only be capable of 10 flights while components of the Crew Launch Vehicle (see Figure 1), based mainly on legacy Shuttle and Apollo technology, will be expendable [35]. These systems are limited by their expendable components and the logistic requirements to ready them for flight.

Military and civilian leaders recognize that there exists a clear need for a responsive launch vehicle for space access [23]. The need to replace the aging, and possibly non-functional, Shuttle fleet has created a newfound political movement for research into next generation RLVs. Additionally, current breakthroughs in hypersonic airbreathing propulsion may hold the key to allowing responsive and high frequency

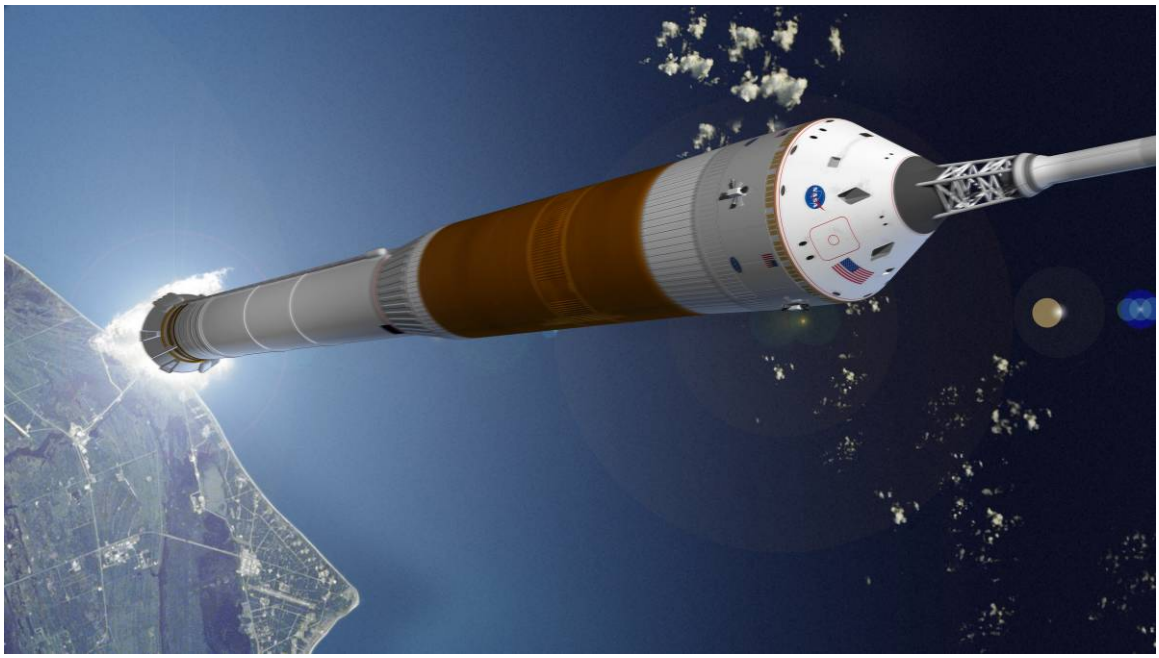

Figure 1. NASA's Crew Exploration Vehicle [35]

access to space. One means of accomplishing this may be through the use of single-stage-to-orbit (SSTO) vehicles.

Unlike two-stage-to-orbit (TSTO) vehicles, SSTOs don't jettison any of their structure, a process known as staging, while ascending to orbit. By not staging, SSTOs are handicapped by the extra weight of their structures and require more powerful, and more efficient means of propulsion. The potential benefits of SSTO include lower maintenance and logistics costs due to the use of one vehicle instead of a system of vehicle components.

The United States may be on the verge of a space renaissance. With the availability of near-term, state-of-the-art technology combined with political will, the promise of low-cost, reliable access to orbit may soon become a reality.

1.2 Research Objectives and Focus

Previous research at the Air Force Institute of Technology (AFIT) has focused on TSTO RLVs using both rocket and airbreathing methods of propulsion [3, 4, 11]. The goal of this study was to analyze the performance of rocket and airbreathing SSTO vehicles, with varying fuel types, and compare their performance to previous TSTO results. This will highlight which propulsion and fuel combinations will be feasible for SSTO RLVs and how they compare to TTSO RLVs of similar configurations. The feasibility of an all-hydrocarbon fuel vehicle was also studied.

Each vehicle configuration studied is unmanned and completely reusable. The vehicle's mission is to launch a 9,071.8 kg (20,000 lbm) payload module with a volume of 79.3 m^3 (2800 ft^3) into a 100 nm circular low-Earth orbit (LEO). Whenever possible,

vehicles' inputs were held constant from configuration to configuration in order to isolate the behavior of a single design parameter at a time. The propulsion systems used in this study include liquid fueled rockets and rocket-based combined-cycle (RBCC) engines. Both systems are analyzed using hydrogen and hydrocarbon fuels exclusively and in combinations. The hydrocarbon dual-mode scramjet (DMSJ) engines used in the RBCC models are derived from research currently being conducted by the U.S. Air Force HyTech program [1].

1.3 Methodology

The Hypersonic System Integrated Design Environment (HySIDE), a program developed by the Astrox Corporation, was used to model the vehicles in this study [14]. HySIDE is capable of modeling the performance of a wide variety of vehicle types using the same analytical methods. This uniform approach incorporates many of the complicated parameters that must be accounted for in hypersonic flight including vehicle dimensions, propulsive forces, fuel consumption, time-varying vehicle mass, aerodynamic forces with hypersonic effects, gravitational losses and temperature effects into one coherent model. This is essential when comparing vehicles with drastically different propulsion methods. HySIDE is capable of incorporating a combination of rocket, turbine, or scramjet engines into a vehicle model and employ them during varying phases of flight. Given a model's input parameters, HySIDE uses an iterative method to size the model and generates performance outputs of the vehicle's size, weight and trajectory.

For ease of understanding, all measurements in this report are given in both metric (SI) and English units.

1.4 Assumptions and Limitations

From the many vehicle parameters used in the design of an RLV, a few parameters were assumed to be the most significant and used as figures of merit in this study. In both aircraft and spacecraft design, a vehicle's empty mass is used as a guide to predict the vehicle's design, materials, manufacturing, quality control and operational costs [2, 21]. Smaller vehicle empty mass is considered favorable. Because of the need to endure large aerodynamic forces under high temperature conditions while re-entering the Earth's atmosphere, the Thermal Protection System (TPS) consumes most of the maintenance cost and man-hours on RLVs [22]. The amount of TPS needed for an RLV is directly related to wetted area, the amount of surface area exposed to the external environment, of the vehicle. Vehicle wetted area is used as another figure of merit for the cost of maintenance and amount of turn-around time needed between launches. Smaller wetted areas are considered favorable.

Compared to the cost of the RLV, the cost of fuel is relatively insignificant [5]. Vehicle gross mass, consisting mostly of mass due to fuel, was therefore not considered to be a major figure of merit in this study. However, because the gross takeoff mass (GTOM) impacts lift-off thrust and launch pad requirements, it is presented in this study.

1.5 Thesis Overview

This work is structured into five chapters and six appendices. Chapter 2 covers background information pertinent to the design and understanding of RLVs, previous RLV programs, research, and the propulsion types analyzed in this study. Chapter 3 clarifies the methodology used in this study. It explains how HySIDE's code works, how mission requirements were derived and how those were used to determine design inputs. Chapter 4 presents the results of this study with an analysis of each vehicle configuration. Chapter 5 discusses the conclusions of this study, how they compare to previous work, and what implications they have to future RLV design.

2. Background Information

This chapter begins by reviewing research done by NASA and the U. S. Air Force in the field of RLVs. The discussion continues with descriptions of the two fundamental means of propulsion for launch vehicles. The third section covers different fuel options for use in RLVs. The fourth section covers the differences between single-stage and multi-stage launch vehicles and the effects on vehicle design. The next section covers the theory behind state-of-the-art airbreathing propulsion methods. The sixth section explores the potential benefits of combining two propulsion methods into one engine and what benefits this may have for SSTO. This chapter concludes with a review of recent research efforts that are pertinent to this study.

2.1 RLV Review

The U.S. Air Force and NASA have pursued research in RLVs since the beginning of the space age. From the development of a sub-orbital space transportation system to the creation of a manned platform for orbital insertion, RLVs have been a major focus of research efforts of both organizations. The most notable endeavors include the X-20 Dyna-Soar, the Space Shuttle, the National Aerospace Plane, the Hyper-X project and NASA's Shuttle-derived Crew Launch Vehicle [24, 30, 31, 32, 36].

2.1.1 Dynamic Soarer (X-20A)

The Dynamic Soarer (Dyna-Soar) project was created in response to the Soviet launch of Sputnik I in 1957. Designed as a military craft for the U.S. Air Force, the

Figure 2. Artist Concept of X-20 Dyna-Soar [26]

Dyna-Soar was intended to be launched aboard a Titan III booster and rendezvous with enemy satellites in orbit. The crew could then inspect the satellite, determine hardware capabilities and possibly disable the satellite before returning to Earth. Figure 2 shows an artist rendition of the upper stage in orbit. Re-designated the X-20 in 1962, the craft measures 10.7 m (35 ft) in length in addition to the Titan III and upper-stage booster. The program was determined to be redundant given NASA's manned spaceflight initiative during the 1960's and the project was terminated in 1963. As one of the first serious looks into lifting-body designs, the Dyna-Soar inspired future X-planes and spacecraft designs [31].

2.1.2 The Space Shuttle

The Space Transportation System (STS) project, more commonly known as the Space Shuttle, was first initiated in 1968 by the Johnson administration. Intended to be a low-cost follow-on to the Apollo program, NASA investigated many different design

Figure 3. Launch of NASA Space Shuttle [27]

configurations for the Shuttle. Under threat of budget cuts by the Nixon administration canceling the program, NASA enlisted financial support from the Air Force in exchange for USAF use of the Shuttle. Deciding upon a TSTO, vertical-takeoff horizontal-landing (VTHL) concept in 1970, the first prototype was completed in 1976. Designated *Enterprise*, the prototype demonstrated the gliding capabilities of the lifting-body design. Using both solid rocket boosters (SRBs), liquid-fuelled rockets and an External Tank (ET), the first operational Shuttle was launched in 1981. The system is not truly a RLV because the ET is expendable. The orbiter and SRBs are the only reusable components. Five shuttle orbiters were built and flown on multiple missions. Figure 3 shows Shuttle *Atlantis* in the first stage of its ascent [24:181-184].

During its lifetime, the Space Shuttle experienced only moderate success in meeting its initial goals. Due to budgetary cuts and design flaws, the orbiter arrived a full 20% more massive than initially designed. This decreased the payload capability and inclination window from continental launch sites. This effectively made the Shuttle incapable of lifting the USAF payloads into polar orbit, a mission that it was designed for

[24]. The Shuttle also failed to reach its launch rate goals. The most launches ever achieved in one year was eleven and occurred in 1985. There were many reasons why the Shuttle's launch rate was limited. However, the most significant factor was the unexpected amount of man-hours required to service and turn-around an orbiter's Thermal Protection System (TPS). The cost of maintaining the Shuttle, in addition to the cost associated with a manned vehicle, inhibited the program from reducing the cost of launching payloads into orbit [15: 433-453]. The Shuttle has also been unable to maintain a regular launch schedule due to technical challenges and two fatal accidents. The *Challenger* accident in 1986 prevented NASA from attaining twelve launches in a single year and halted Shuttle operations for two years. The loss of *Columbia* in February of 2003 caused another stop in operations, crippling the construction of the International Space Station (ISS). Even after the first post-*Columbia* flight two and a half years later, the ability of the aging Shuttle fleet to safely carry out its mission is in question.

2.1.3 National Aerospace Plane (X-30)

Initiated in 1986 during the Regan administration, the National Aerospace Plane (NASP) proposed to offer a civilian means of transportation that could, "take off from Dulles Airport and accelerate up to twenty-five times the speed of sound, attaining low earth orbit or flying to Tokyo within two hours..." [30]. Designated the X-30 by the military, the NASP was a Phase II follow-on to a classified Defense Advanced Research Project Agency (DARPA) program during the early 1980's. Over the next eight years, NASA and the Department of Defense spent $3.33 billion on producing technologies and

designs for the NASP. The conceptual design, shown in Figure 4, consisted of a scramjet-powered, SSTO craft that took off and landed horizontally. The horizontal configuration was necessary for the craft to be used routinely by civilian assets.

The NASP was the first design to incorporate actively cooled surfaces. This design system and process pumped cold fuel under surfaces that experienced extreme heating from drag in hypersonic flight before injecting the fuel into the engine. This design process enables higher speeds and increases the efficiency of the combustion in the engine. However, the hardware to enable this form of active TPS results in a significant weight penalty. Initially attempting to attain a maximum speed of Mach 25 under airbreathing propulsion, technical problems and the weight of the active TPS reduced this design requirement to Mach 20, and then further to Mach 17. External rockets would be needed to achieve orbit. Skyrocketing cost projections and insurmountable technical challenges prevented the project from reaching Phase III with an operational vehicle. Over time, the program died out. However, the Hypersonic Systems Technology Program (HySTP) was created as a joint DOD/NASA initiative to catalog and implement the wealth of technologies developed during the NASP project. In

Figure 4. National Aerospace Plane Concept [29]

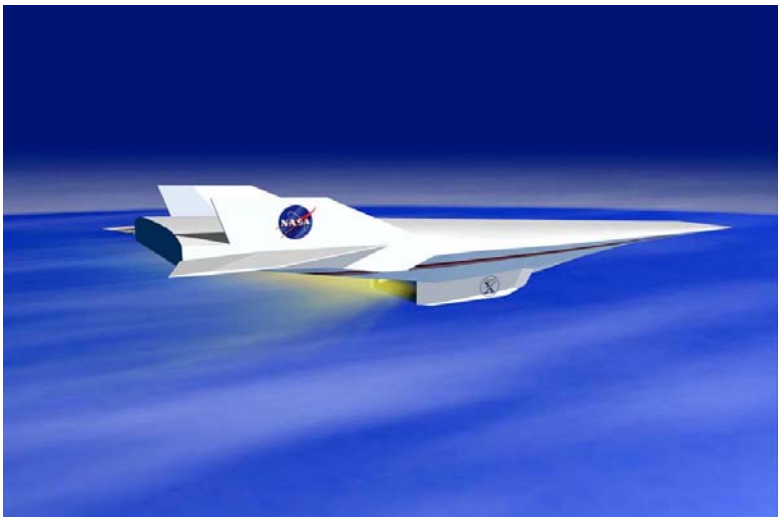

Figure 5. Computer Image of X-43A in Flight [36]

1995, the Air Force withdrew its participation from HySTP, marking the official end of the NASP program [30].

2.1.4 Hyper-X (X-43) and HyTech

NASA, along with the USAF, established a program to demonstrate airbreathing engine technology that has the capability to power the next generation of U. S. spacecraft and possibly allow for SSTO vehicles with sizable payloads. After substantial design and wind tunnel testing, the Hyper-X program peaked with the successful testing of two unpiloted vehicles. Powered by NASA-developed hydrogen scramjets, the X-43A craft set the world speed record for airbreathing aircraft (the previous record holder was the SR-71 Blackbird at Mach 3.1) by achieving a velocity of Mach 9.6 [32, 36]. The vehicles, shown in Figure 5, proved the viability of scramjet propulsion. However, NASA's reallocation of assets in accordance with President Bush's manned spaceflight directive, has forced the agency to focus on near-term development of a production spacecraft. It was determined that SSTO was un-attainable within that timeframe and NASA dropped its support of scramjet research [8].

The U. S. Air Force is currently conducting research and development into the production of a scramjet using hydrocarbon fuel. Established in 1995, the Hypersonic Technology (HyTech) program is leveraging off the success of the Hyper-X initiative. The project is currently looking at TSTO RLVs for use in military applications, such as responsive space access, and hopes to field a vehicle by 2014 [20:9].

2.1.5 Crew Launch Vehicle (CLV)

In accordance with President Bush's vision for manned space exploration, NASA is currently developing a launch vehicle to get personnel and equipment into orbit, to the Moon and to Mars. The Shuttle-derived Crew Launch Vehicle uses existing technology to create a safe and reliable platform for space launch. By using a larger Shuttle SRB, modified ET and a Saturn V upper-stage booster, the CLV should have minimal developmental costs. As the designated replacement for the Shuttle, the CLV will be the flagship of NASA's manned spaceflight program for the foreseeable future.

2.2 Basic Propulsion Options

All aircraft and spacecraft propulsion methods rely on the same basic principle: producing thrust by expelling mass, or propellant usually in the form of a gas, out the back of the vehicle to produce thrust. The two basic types of propulsion suitable for launch vehicle are rocket engines and airbreathing engines. Currently, all launch vehicles use rocket propulsion. High-speed airbreathing propulsion methods remain at the cutting edge of state-of-the-art and near-state-of-the-art technology.

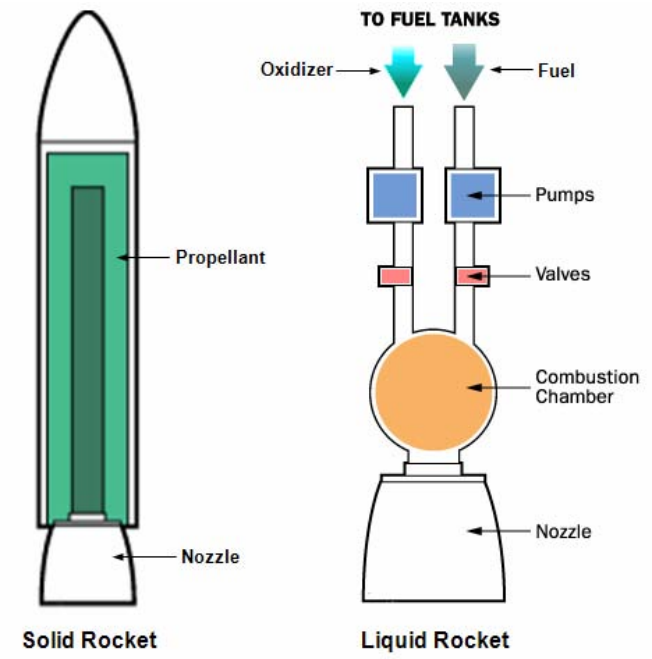

Figure 6. Solid and Liquid-Fuel Rocket Engine Operation [34]

2.2.1 Rocket Propulsion

Rocket propulsion is one of the simplest forms of producing thrust. First invented in China, rockets have a long history dating back hundreds of years [34]. Thrust is created by expelling combusted hot gas through a nozzle in the direction opposite of flight. The combustion reaction in achieved through the burning of a fuel and an oxidizer which are both carried onboard the vehicle. Rockets engines can either use liquid or solid propellants (Figure 6).

Solid rockets combust a solid compound that burns very quickly, but does not explode, inside a fixed-volume container. As the propellant burns, it expands and increases the pressure inside the chamber. This pressure forces combusted propellant, now in the form of a hot gas, out through the nozzle at a high rate of speed. On the other hand, liquid rockets store the propellants separately and then combine them just prior to combustion. Generally, solid rockets are simpler than liquid rockets. They do not

require the machinery to pump and mix propellants nor do they need heavy fuel tanks. Solid rockets do lack the capability to throttle, stop or re-start unless sophisticated design elements are included. Liquid rockets have the ability to control the thrust output in flight. One drawback of liquid rockets is that the propellants are usually cryogenic or toxic requiring special handling and ground maintenance. Solid propellants are usually inert until ignited.

2.2.2 Airbreathing Propulsion

Airbreathing engines differ from rockets in that they obtain all the oxidizer for combustion from the atmosphere. This means that an oxidizer does not need to be carried onboard the craft which has the potential to make the vehicle lighter. However, this restricts these engines to only operate where ambient oxygen is available, thus making them incapable of extra-atmospheric operations. Airbreathing propulsion engines have higher specific impulses than rocket engines. While airbreathing engines have been used almost exclusively in aircraft, new technologies may enable them to be used for RLVs. During ascent, RLVs spend a large amount of time in the atmosphere where ambient oxygen is plentiful, During these phases of flight, airbreathing propulsion methods could be used to accelerate an RLV up and out of the atmosphere more efficiently than conventional rockets. However, once the density of the atmosphere reaches a minimum value, rocket propulsion will have to take over to accelerate an RLV the rest of the way to orbit.

The two types of airbreathing propulsion most applicable to SSTO RLVs are ramjets and scramjets. Ramjets are the simplest jet engines because they have no moving

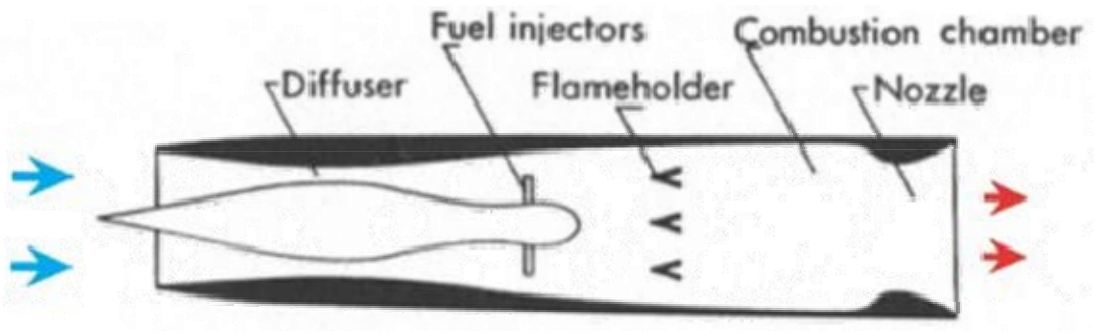

Figure 7. Diagram of Scramjet Operation [34]

parts (Figure 7). Air enters the engine and is compressed through a series of shock waves to sub-sonic speeds. Fuel is mixed with the air and then ignited, accelerating the burning mixture out the nozzle. At high supersonic speeds, the engines used on the SR-71 Blackbird operated in a ramjet mode, bypassing the unneeded components of the engine, using the afterburner alone. Because ramjets require the forward velocity of the vehicle to compress the air, they can only operate at high speeds and operate most efficiently above Mach 3. The need to decelerate the incoming air to subsonic speeds prevents ramjets from being effective above Mach 6 [12:154-157].

A scramjet, supersonic combusting ramjet, is a variation on the ramjet design that allows the flow to combust while still supersonic. By not needing to reduce the flow to sub-sonic speeds, scramjets are not limited to Mach 6 like ramjets. However, properly mixing and reacting the incoming supersonic air and fuel can be difficult due to the high speed of the flow. Theoretically, scramjets are capable of achieving speed of up to Mach 15 [12:263-264]. Engines that are capable of operating as both ramjets and scramjets, dual-mode scramjets (DMSJ), are being researched by the HyTech program and will be able to operate over the entire speed range of Mach 3 – Mach 15 [20].

2.3 Fuel Options

Most of the mass of a spacecraft is taken up by the propellant. Therefore, which type of propellant used can have a major impact on the size, shape and performance of an RLV. The two most common fuels used are liquid hydrogen (LH_2) and hydrocarbons such as RP-1. Hydrogen is generally more powerful because it contains more energy per unit mass than hydrocarbons. However, hydrogen is less dense than hydrocarbons and therefore takes up a larger volume. This increases the weight of fuel tanks and the aerodynamic drag due to a larger vehicle. Hydrogen must also be stored in liquid form at cryogenic temperatures requiring cooling capabilities and insulation. These translate into more weight penalties for the vehicle as well as increased ground service and support equipment and personnel to maintain cryogenic storage. Hydrocarbons are able to be stored at near-room temperatures and don't require these considerations. For civilian applications and responsive military requirements, hydrocarbon fueled RLVs are favorable over vehicles that require hydrogen [17].

2.4 SSTO vs. TSTO

Two-stage-to-orbit launch vehicles reduce mass during ascent by discarding propellant and structure. The point at which the vehicle expends a portion of its structure is called staging. Single-stage-to-orbit launch vehicles only discard propellant on their way to orbit. For a SSTO, there is an exact trade-off between structural mass and payload mass. SSTO vehicles are very sensitive to vehicle dry mass and its reduction is critical. In the past, the lack of certain technologies has made the feasibility of SSTO vehicles questionable. By staging, a TSTO vehicle reduces its structural mass during the

last phases of flight. This opens the margin of performance to a feasible level for attaining orbit. New advances in propulsion and material science have increased the efficiency of engines and allowed for smaller structural mass fractions. These new developments may put SSTO within reach [19:3].

SSTO vehicles have some potential benefits over multi-stage launch systems. By combining the system into one vehicle, SSTOs are more operationally flexible because they do not require the assembly of multiple vehicle components. Also, SSTO vehicles may have smaller wetted areas, and thus a lower amount of maintenance-demanding TPS, reducing the maintenance hours required to turn around a RLV after returning from orbit. While these benefits make SSTO RLVs appealing, multi-stage launch vehicles have been standard for over forty years. Industry is familiar with these systems and the design architecture is focused around this main feature.

2.5 Airbreathing Propulsion in RLVs

The largest debate currently among researchers in RLVs is between the use of rockets or airbreathing forms of propulsion. Rockets have been used for decades and are very well understood. However, emerging airberathing propulsion technology may prove to be more efficient than rockets and eventually augment rockets on space launch vehicles.

2.5.1 Airbreathing Propulsion Advantages

Airbreathing propulsion's most notable advantages over traditional rocket propulsion include higher specific impulse, decreased sensitivity to increases in inert

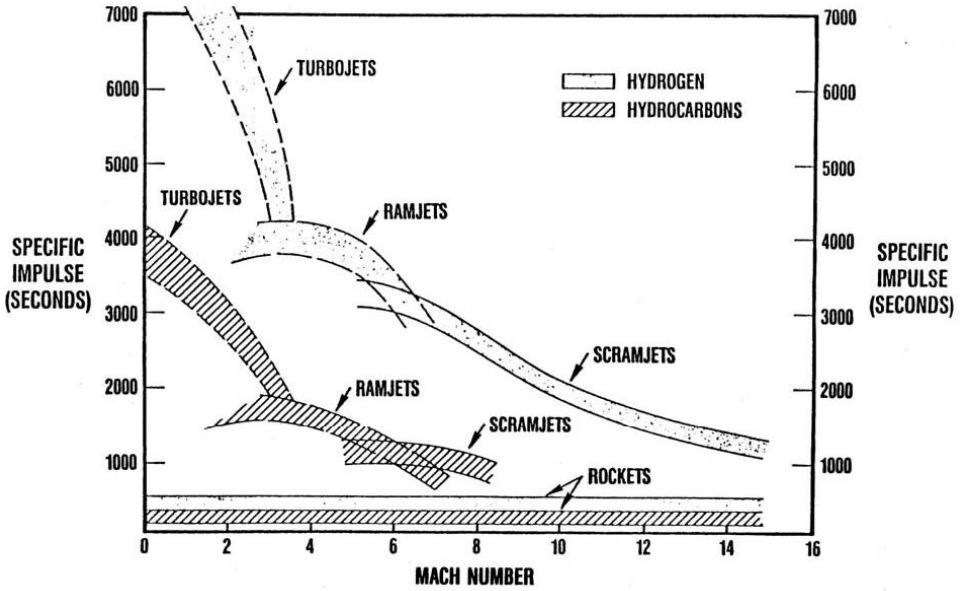

Figure 8. Specific Impulse vs. Mach for Different Propulsion Types [9]

mass and greater safety. By using the oxygen in the atmosphere, airbreathing propulsion does not need to carry oxidizer in the vehicle. The largest consequence of this is a larger specific impulse (I_{sp}) than rockets. Specific impulse is a measurement of the amount of thrust produced for a given flow rate of propellant expelled. In rockets, this propellant is the sum of fuel and oxidizer, while in airbreathing engines, only the fuel is counted because the atmospheric oxygen is not considered onboard propellant. Higher specific impulses are analogous to higher efficiencies. A typical rocket will have an I_{sp} between 300 and 500 seconds. As shown in Figure 8, airbreathing engines are capable of reaching specific impulses in excess of 7000 seconds. Because of their specific impulse, airbreathing engines can produce the same amount of thrust as a rocket engine but use less propellant. This drastically decreases the gross and inert mass of a vehicle.

Because they require less propellant per mass of structure and payload, airbreathing vehicles are less susceptible to vehicle growth due to increases in inert mass. In SSTO vehicles, this advantage balances with the extra sensitivity SSTOs have to weight growth. Susceptibility to weight growth is a good indicator of the quality of a

vehicle's design. On most vehicles, inert mass increases over time as newer systems are added on, mission capabilities expanded and flexibility increased. Reducing sensitivity to weight growth is fundamentally key to designing a successful vehicle.

Because of their design, airbreathing propulsion methods are more reliable than rocket-based ones. Airbreathing engines operate at lower chamber pressures resulting in greater reliability and service life. Of all launch failures, many are a result of propulsion system failures [19]. Increasing the safety of the engines is essential to maintaining overall system reliability. When a failure does occur, airbreathing engines are less prone to catastrophic failures than rockets. With manned missions, this allows the crew time to escape given a total failure of the propulsion system.

2.5.2 Airbreathing Propulsion Disadvantages

While the benefits of using airbreathing propulsion are numerous, there are some drawbacks including technical complexity, limited operability in altitude and air speed, engine weight and other weight penalties associated with airbreathing vehicles. These drawbacks are the reasons why no space launch system has yet to use airbreathing propulsion. Airbreathing propulsion is insufficient to take a vehicle all the way to orbit. They are unable to operate in the oxygen-deprived environment of the extreme upper atmosphere and are restricted to the lower portions of a vehicle's trajectory. Additionally, each form of airbreathing propulsion can only operate over a specified speed range. For ramjets and scramjets, another means of propulsion must be used to accelerate the vehicle to the minimum usable Mach number for those engines.

Airbreathing propulsion only works during the middle segment of an ascent when the vehicle is within a specified speed and there is still enough ambient oxygen.

While airbreathing vehicles have advantages in gross mass, they are less advantageous in terms of vehicle empty mass. Compared with rockets producing the same thrust, airbreathing engines weigh more. This reduced thrust-to-weight is due the mechanics of airbreathing engines. Because of their flight profile spends more time in dense air at high speed, airbreathers require a more robust TPS. Rockets on the other hand, ascend very quickly, and spend little time in the dense portions of the atmosphere thus reducing vehicle heating due to drag.

The shape of the launch vehicle is also important. Rockets can conform to the highly efficient cylindrical shape they exhibit today. This grants reduced drag, straightforward structural support and efficient shapes for the fuel tanks. With airbreathers, the outer surface of the vehicle must act as both the compressor and nozzle. This restriction generates a vehicle shape similar to that shown in Figure 9. This shape is not as drag efficient as a cylinder/ogive and the most effective means of shaping and placing fuel tanks is still unknown. These factors all constitute penalties in the empty mass of an airbreathing vehicle that oppose the benefits achieved by an airbreather's large specific impulse.

2.6 Combined-Cycle Propulsion

Rockets are robust and can operate at all altitudes and all speeds, while airbreathers are highly efficient. A hybrid engine, combining the best aspects of both propulsive means, is possible. These combined-cycle engines have the ability to

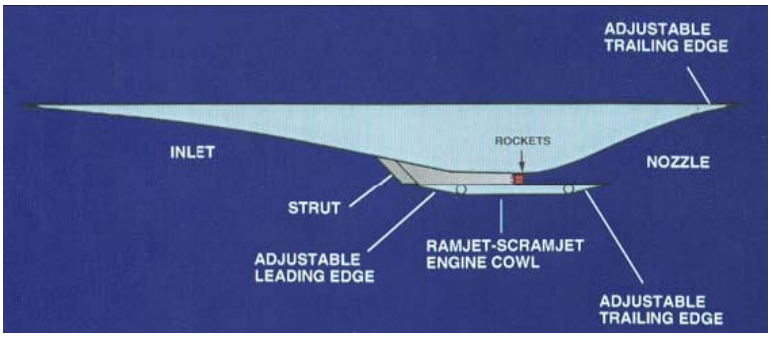

Figure 9. Diagram of RBCC vehicle [28]

implement either method of producing thrust based on which is both possible and most efficient at the time. Rocket-based combined-cycle (RBCC) engines combine a DMSJ with a liquid rocket into one platform (see Figure 9). This configuration allows the use of a rocket to accelerate a vehicle from rest to the minimum velocity needed to initiate ramjet propulsion. Then the engine stops using its own oxidizer and switches over to ram-scramjet mode using onboard fuel and ambient air to accelerate the vehicle to the limiting maximum attainable speed or altitude. The RBCC then switches back to rocket-mode and boosts the vehicle the rest of the way to orbit [11].

2.7 Recent RLV and SSTO Research

There has been a great deal of research recently in the field of RLVs. New technological advances have opened the door to new possibilities such as airbreathing propulsion and SSTO. Eight separate studies are summarized here: three by the Air Force Institute of Technology (AFIT) [3, 4, 11], two by NASA [19, 25], one by the Astrox Corporation [5], one by the Air Force Aeronautical Systems Center [18] and one by the University of Maryland [7].

2.7.1 NASA Abort Performance Study (1995)

This study investigated the abort-to-orbit (ATO) and return-to-launch site (RTLS) capabilities of a rocket-powered SSTO vehicle. The study first sized a SSTO vehicle that could carry a 9,071.8 kg (20,000 lbm) payload module into LEO. The study settled on a winged-body design powered by seven LH_2 fueled Space Shuttle main engines (SSME). The gross take off mass and empty mass of the vehicle were 1,081,106 kg (2,383,430 lbm) and 93,667 kg (206,500 lbm) respectively. The study concluded that the vehicle had acceptable abort capability in one- and two-engine-out scenarios [19].

2.7.2 NASA Lawrence Livermore Study (1996)

A study conducted at the Lawrence Livermore Lab evaluated the trade considerations between fuel types in SSTO rocket applications. The goal was to determine the effects of specific impulse and fuel density on tank size, engine size, propellant weight fraction, and orbiting mass fraction. The study found that the selection of fuel type greatly affects the mass allocation of a vehicle. Findings lead to the conclusion that hydrocarbon fuel SSTO rockets will have a lower empty weight fraction than hydrogen fuel SSTO rockets. The study also concluded that tri-propellants theoretically offer weight fraction advantages over bi-propellant rockets [25].

2.7.3 AFIT Reusable Launch Vehicle Study (2004)

This study looked at TSTO launch vehicles using rocket, turbine and RBCC engines. It analyzed five different RLV configurations with a fixed gross weight of one million pounds using NASA's Program to Simulate Trajectories (POST). The study

concluded that payload and inert weights were most sensitive to stage structural weight fractions for rockets. It also found that when using a turbojet on the first stage, horizontal takeoff was preferable to vertical takeoff because turbojets don't have enough thrust for practical vertical takeoff. Additionally, the study found that RBCC engines should not follow direct-ascent trajectories like rockets but a constant dynamic pressure trajectory instead. The study found that of all the RLV configurations, using a rocket on both stages had the best performance [3].

2.7.4 Astrox Reusable Launch Vehicle Study (2004)

Using their design tool, HySIDE, the Astrox Corporation compared TSTO rocket RLVs with SSTO RBCC RLVs using hydrogen, hydrocarbon and tri-propellants. Empty weight was used as a figure of merit. Each vehicle was sized to lift a 9,071.8 kg (20,000 lbm) payload module. The HySIDE program was used to analyze each vehicle in the same manner and model the vehicles through their entire flight profiles. The study found that for SSTO, taking off vertically resulted in a lighter craft that taking off horizontally. This was due to the extra wing and gear weights needed when taking off horizontally. The study also found that improvements in airbreathing technology were essential to the development of SSTO vehicles. For the rocket TSTO RLVs, using tri-propellants resulted in the lightest weight [5].

2.7.5 Aeronautical Systems Center Study (2004)

This study looked at TSTO and SSTO RLVs in a variety of configurations. Both vertical and horizontal takeoff systems were analyzed using empty weight, growth factor

and wetted area as figures of merit. The study concluded that there currently exist numerous reusable and hybrid (partially reusable) systems that are technically achievable with current technology. It also pointed out that future technical innovations must focus on increasing the operability of RLVs. Horizontal takeoff vehicles proved to be heavier than vertical takeoff systems and were not recommended for development. The study also showed that turbine-based vehicles were not advantages and should not be used to achieve "aircraft-like" operations. The study suggested that, to achieve access to space, efforts should focus on vertically launched RBCC systems with an eye on eventually achieving SSTO [18].

2.7.6 AFIT Reusable Launch Vehicle Weight Study (2005)

This study investigated RLVs in three areas using POST and HySIDE and empty weight as the figure of merit. The first area compared the following TSTO configurations: rocket-rocket, turbojet-rocket, TBCC-rocket and RBCC-rocket. Like the 2004 study, the all rocket vehicle was the lightest launch vehicle. The TBCC-rocket was the second lightest. Another area considered was a fuel comparison between hydrogen and hydrocarbon. Little difference was observed for VTHL configurations, but hydrogen was significantly lighter in HTHL configurations. A thrust-to-weight comparison was also conducted on the TBCC and turbojet configurations. Increasing the thrust to weight ratio naturally reduced the empty mass of the vehicle. This study used rockets on all of the orbiter stages but recommended looking at placing an RBCC as a second stage [4].

2.7.7 University of Maryland Study (2005)

Looking at both SSTO and TSTO, this study combined empty weight, wetted area and maintenance hours as figures of merit. The comparison baseline consisted of both hydrogen and hydrocarbon versions of a TSTO rocket-rocket. The study found that placing hydrocarbon on the lower rocket stage and hydrogen on the upper rocket stage increased performance. These were then compared with airbreathing models in both vertical and horizontal takeoff configurations. In HTHL, a turbine-RBCC configuration was the lightest and had the least wetted area. All the VTHL vehicles were lighter than their HTHL counterparts. Inward turning and 2-D geometries were considered for the RBCC's. The study found that inward turning geometries were lighter, had less area than, and experience less heating than their 2-D counterparts [7].

2.7.8 AFIT TSTO Reusable Launch Vehicle Study (2006)

This study compared 27 separate vehicle configurations for TSTO RLVs using turbine, TBCC, RBCC and rocket propulsion methods in VTHL and HTHL configurations. Empty weight and wetted area were used as orders of merit. The different configurations flew multiple types of missions including orbital insertion, orbital rendezvous, and global strike. The study found that using airbreathing propulsion on the upper stage resulted in weight savings. The best configuration for HTHL was a hydrocarbon TBCC-hydrogen RBCC and for VTHL was an all-hydrocarbon rocket-RBCC. This study also refined values of lift coefficient, lift-over-drag and scramjet specific impulse [11].

3. Methodology

This chapter discusses the methods used in this study, how RLVs models were constructed and what assumptions were made. A variety of models were built using Astrox Corporation's HySIDE, a parametric hypersonic vehicle sizing code, the results of which are presented in the following chapter. HySIDE was designed to offer flexibility in vehicle design and simultaneously track a multitude of variables affecting vehicle performance including aerodynamic forces, hypersonic effects, heating effects, propulsion performance, gravity losses, vehicle volume and mass [14]. VTHL SSTO RLV models using conventional liquid rocket or RBCC propulsion employing hydrogen, hydrocarbon or both fuel types were constructed and analyzed. Each model was sized for launch of a 9,071.8 kg (20,000 lbm) payload module into a circular 100 nm orbit, then de-orbit, re-enter the atmosphere and land. Vehicle susceptibility to payload uncertainty was investigated to determine the operational robustness of each system.

3.1 SSTO RLV Configurations

The vehicles in this study are all single-stage-to-orbit, carrying all the initial structural weight through the entire ascent and decent. Neither external boosters nor secondary vehicles were used on these systems. Each vehicle contains a propulsion system, propellant, tank structure, payload module, landing gear, lifting and control surfaces, an Orbital Maneuvering System (OMS), and the structure needed to support these components. Like the upper stage of TSTO RLVs, the entire SSTO vehicle must

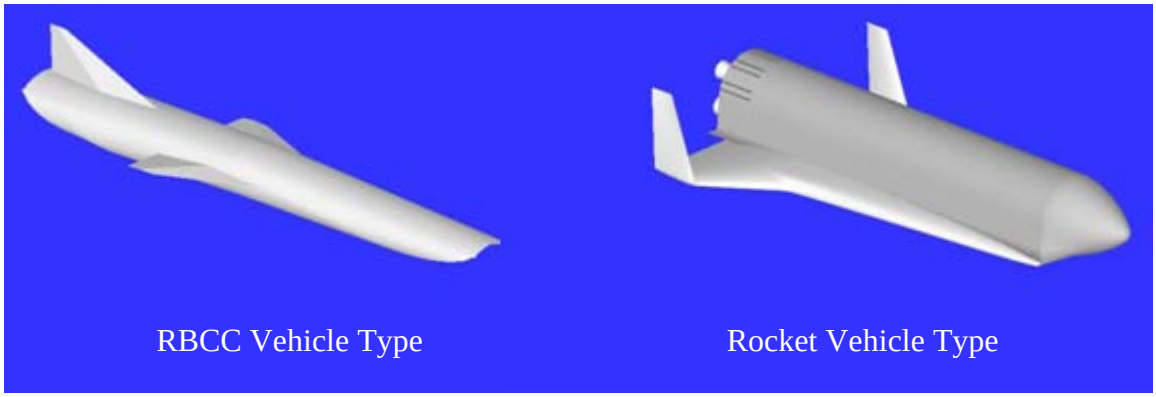

Figure 10. SSTO RLV Types

undergo re-entry and requires both active and passive Thermal Protection Systems (TPS). The two types of vehicles considered, rockets and RBCCs, are shown in Figure 10.

For RBCC vehicles, the flight profile consists of three segments. The first segment is rocket-powered and accelerates the vehicle off the launch pad to the minimum speed for the DMSJ to operate. The second segment uses the DMSJ to accelerate the vehicle further. The third segment is rocket-powered and takes the vehicle all the way to orbit. This segment begins when the effective specific impulse (EI_{sp}) of the DMSJ drops too low and it becomes favorable to use the rocket, or the heating on the DMSJ becomes too great (discussed later). Each of these segments can use hydrogen or hydrocarbon fuel. SSTO rockets' only segment is a direct ascent to orbit and can also use either hydrogen or hydrocarbon for fuel. Two special fuel options were considered: a tri-propellant rocket and a bi-fuel mixture DMSJ. These different fueling and propulsion options result in the 9 basic models shown in Table 1. Each vehicle is designed for a VTHL configuration. Past studies have shown that HTHL SSTOs are much heavier than their VTHL counterparts and therefore were not considered in this study [18].

Table 1. RLV Fuel Options

Rocket Model Fuels
H
HC
HC / H

RBCC Model Fuels		
Rocket Mode	DMSJ Mode	Rocket Mode
H	H	H
HC	H	H
HC	HC / H	H
HC	HC	H
HC	HC	HC
H	H	HC
HC	H	HC

H - Hydrogen HC - Hydrocarbon

Due to convergence difficulties, the RBCC model using hydrogen-hydrogen-hydrocarbon fuel options could not be included in this study. Four TSTO models were included for comparison from the 2006 AFIT RLV study [11].

The orbital parameters at Main Engine Cutoff (MECO) are a velocity of 7,468.5 m/s (24,503 fps), perigee of 50 nautical miles (nm) or 92.6 km (303,800 ft), apogee of 100 nm or 185.2 km (607,612 ft), and an inclination of 28.6°. The launch site was assumed to be Kennedy Space Center (KSC). Once at apogee, an OMS burn is used to circularize the orbit at 100 nm. Once the payload is deployed, the vehicle conducts another OMS burn and reenters the atmosphere for landing.

3.2 Flight Fundamentals

As an RLV moves through the atmosphere, the forces acting on it determine its motion. These forces can be divided into body forces and aerodynamic forces. Aerodynamic forces include the lift (L) and drag (D) due to pressure variations on the vehicle's surface. Body forces include the force due to the Earth's gravity, or weight (W), and the thrust (T) produced by the vehicle's engines. These forces are shown on a RLV in Figure 11.

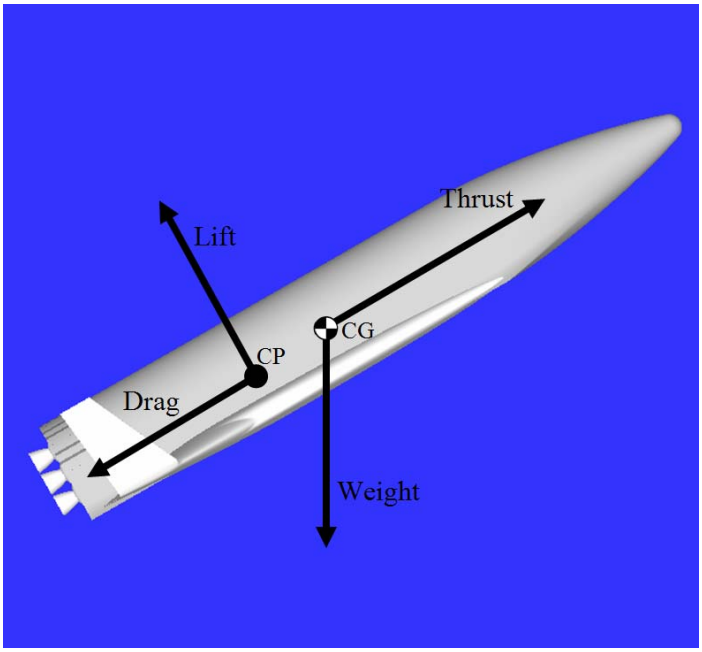

Figure 11. Forces on RLV

3.2.1 Aerodynamic Forces

These forces result from the varying pressure distribution of the environment on the surface of the RLV. The components of the resulting force can be broken into lift and drag. Lift is the component of the pressure force that acts perpendicular to the relative wind direction and drag acts parallel to the relative wind velocity. These two force components, which are derived from a force distribution, act on the vehicle from the center of pressure (CP). For convention, both lift and drag can be described with the lift coefficient (C_L) and drag coefficient (C_D). The relationships between the forces of lift and drag and their non-dimensional coefficients are

$$L = C_L \cdot q \cdot S_{ref} \tag{1}$$

$$D = C_D \cdot q \cdot S_{ref} \tag{2}$$

$$q = \frac{1}{2} \cdot \rho \cdot V^2 \tag{3}$$

where q is the dynamic pressure of the flow, S_{ref} is the reference wing area of the vehicle, ρ is the density of the fluid, and V is the velocity of the vehicle relative to the fluid. Values of C_L and C_D were taken from the 2006 AFIT Study where a detailed analysis of these values was conducted [11].

3.2.1 Body Forces

The weight of the vehicle changes linearly as the mass of the vehicle decreases during flight due to propellant mass flow. The relationship between weight and mass is given by

$$W = m \cdot g \tag{4}$$

where m is the total mass of the vehicle at any instant and g is the acceleration due to the Earth's gravity. Regardless of the vehicle's orientation, gravity always acts downward towards the Earth's center through the vehicle's center of gravity (CG). During the ascent of a launch vehicle, momentum is lost due to gravity. This effect is called gravity losses and is related to the amount of time it takes for a vehicle to reach orbit. The following relationship defines gravity losses as

$$G_{losses} = m \cdot g \cdot \frac{\Delta h / \Delta t}{V} \tag{5}$$

where Δh is the change in altitude from launch to orbit, Δt is the time to orbit and V is the vertical velocity [13].

Thrust is used to accelerate a vehicle from rest at the Earth's surface to orbital velocity in space. Both rocket and airbreathing vehicles produce thrust by accelerating propellant out the back of the engine. In the case of rockets, the propellant is initially at

rest with respect to the vehicle. The thrust produced is the sum of the momentum change of the propellant by the engine and the pressure losses due to atmospheric back-pressure. For a rocket, the thrust is

$$T_{rocket} = \dot{m}_{propellant} \cdot V_{exit} + \left(P_{exit} - P_{atm} \right) A_{exit} \tag{6}$$

where $\dot{m}_{propellant}$ is the mass flow rate of the propellant through the engine, V_{exit} is the velocity of the propellant as it exits the engine, P_{exit} is the pressure of the propellant as it exits the engine, P_{atm} is the ambient pressure of the atmosphere and A_{exit} is the area of the engine's exit plane [13:110].

For airbreathing engines, some of the mass being accelerated and expelled through the engine's exit is not entering the engine from relative rest. The momentum of the air coming into the engine must be accounted for, resulting in the following relationship:

$$T_{rocket} = \dot{m}_{exit} \cdot V_{exit} - \dot{m}_{air} \cdot V_{air} + \left(P_{exit} - P_{atm} \right) A_{exit} \tag{7}$$

where $\dot{m}_{exit}$ is the combined mass flux of the exiting propellant and exiting air that has been accelerated by the engine, $\dot{m}_{air}$ is the mass flow of the incoming air from the atmosphere, and V_{air} is the velocity of the air coming into the engine [12:148].

Two parameters are used when rating and comparing the performance of engines, specific impulse (I_{sp}) and specific fuel consumption (*SFC*). I_{sp} is the measure of the amount of thrust produced per mass of propellant expelled and is defined by:

$$I_{sp} = \frac{T}{\dot{m}_{propellant} \cdot g} \tag{8}$$

The factor g is an arbitrary constant that produces I_{sp} in units of seconds. In rockets, $\dot{m}_{propellant}$ is the mass of the fuel and the oxidizer that are stored in the vehicle's tanks and then accelerated through the engine. For airbeathing engines however, $\dot{m}_{propellant}$ is only the mass of the fuel that the engine burns. The I_{sp} of airbreathers doesn't include the mass flow of the oxidizer (or air), because it is not carried onboard the vehicle, and is the main reason why the I_{sp} is so high compared to that of rockets. Engines with high I_{sp} are analogous to engines with higher efficiencies. This is where airbreathing propulsion methods outperform rocket engines.

Specific fuel consumption (SFC), another rating of engine efficiency, measures the amount of fuel burned per time of burn and per amount of thrust produced. In *SFC*, lower values are favorable and are defined by the equation

$$SFC = \frac{W_{propellant} / t}{T} \tag{9}$$

where $W_{propellant}$ is the weight of the propellant burned over time (t) and T is the thrust produced. *SFC* can be expressed in units of $N/N \cdot s$ $\left(lbf/lbf \cdot s\right)$, or $1/s$, or more commonly $1/hrs$. Specific impulse is more commonly used to rate rocket engine performance while specific fuel consumption has been historically used to rate airbreathing engines. This study uses specific impulse for all propulsion methods. To convert between *SFC* and I_{sp}:

$$I_{sp} = \frac{3600\ s/hr}{SFC} \tag{10}$$

Because thrust directly opposes gravity and drag, specific impulse can be presented as an effective specific impulse or EI_{sp} and is defined as:

$$EI_{sp} = I_{sp} - \frac{D}{\dot{m} \cdot g} - \frac{G_{losses}}{\dot{m} \cdot g} \tag{11}$$

3.3 HySIDE Design Methodology

The Astrox Corporation's Hypersonic Integrated Design Environment (HySIDE) was used to model, size and analyze the vehicles in this study. The 2006 AFIT TSTO study was consulted for this entire section [11]. The program allows a user to combine separate components into a complete vehicle model. This modular design

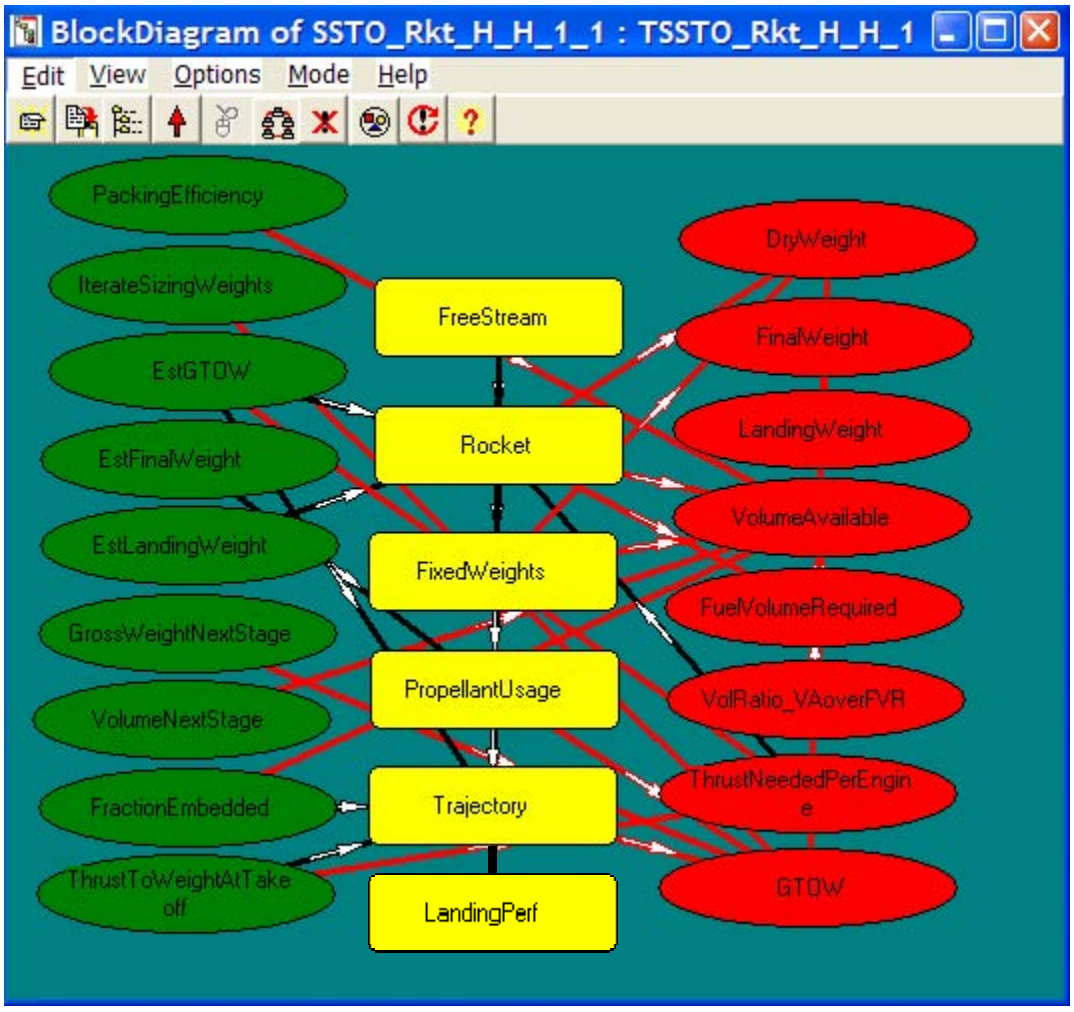

Figure 12. HySIDE Model Block Diagram

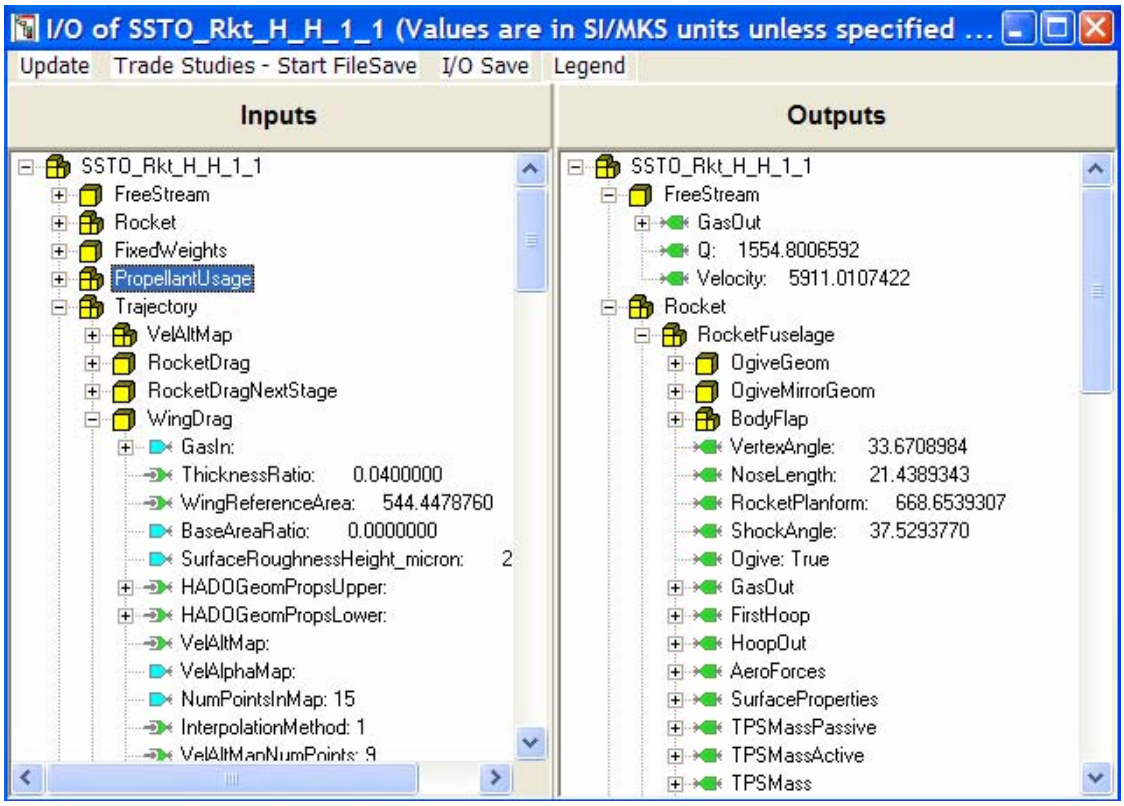

Figure 13. HySIDE Model System Tree

allows for the analysis of a wide range of vehicle types using similar methods of analysis. HySIDE employs an integrated analysis approach where the many design variables are accounted for simultaneously. For every vehicle in this study, there are six main components, called system elements or "SysEls", that make up the model: FreeStream, Rocket or HADOVehicleBasic, FixedWeights, PropellantUsage, Trajectory, and LandingPerf. Using the graphical user interface (GUI) shown in Figure 12, a user can assemble these different SysEls into a complete vehicle model. Inputs into the model are shown in green and outputs are shown in red. Each of these six SysEls are composed of additional SysEls which have their own inputs and outputs. The user can control the inputs to the model in the input/output (I/O) window shown in Figure 13. This collapsible tree representation mirrors the structure of the model's block diagram.

To size a vehicle, a user enters in all the inputs that apply to the model (some of which are discussed later) and then runs the sizing code. This process uses an imbedded subroutine to estimate the vehicle's gross takeoff mass (GTOM) based on the user-defined size parameter inputs. The code then "flies" the vehicle through the trajectory the user specifies. At the end of the trajectory, the code calculates the total propellant that was required and compares this to the estimated amount of propellant and estimated vehicle size. If the estimated vehicle size differs from the required vehicle size, an iterative process begins where the code makes a new GTOM guess, runs through a simulation, continuing until the vehicle size converges and the change is below a tolerance determined by the user (in this case 0.01%). Once the model has converged, the code compares the volume of the vehicle with the required volume for the tanks, payload and other internal components. This ratio is calculated and displayed as the "VoRatio_VAoverFVR" dependant variable in model outputs. This value must be greater than unity for the model to be accurate; there must be at least enough volume inside the vehicle to contain all the vehicle's components. If this output is less than unity, the user must increase the model's dimensional parameters (thus making the vehicle larger) and re-run the sizing code. Likewise, if there is substantially more available volume than required, the user should decrease the vehicle dimensions and resize the vehicle. Ideally, the volume ratio should be greater than unity by 1 - 2%.

The model input "PackingEfficiency" has a major effect on the required volume of the vehicle. This input specifies the how well the propellant tanks and payload module fill the available volume. For complicated vehicle shapes, like those found on an inward-turning RBCC, there is a great deal of uncertainty in how well cylindrically-based tanks

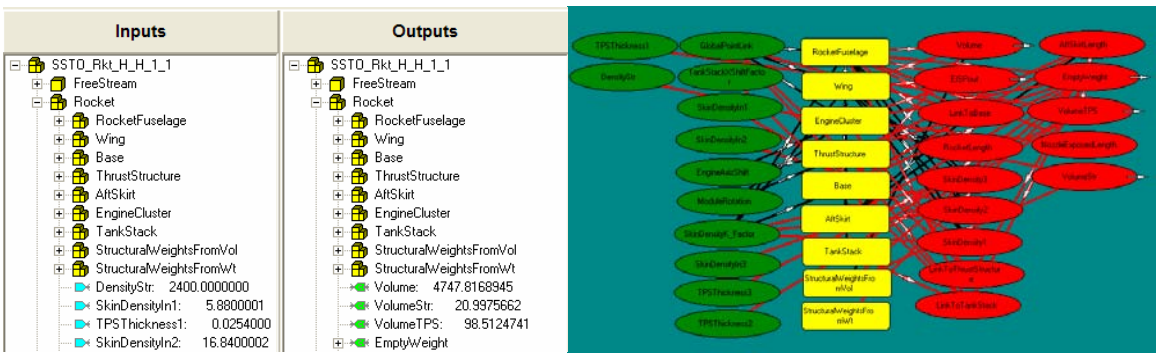

Figure 14. Rocket System Element and I/O

will conform and fill the available volume. In this study, a "PackingEfficiency" of 0.85 was used for airbreathing vehicles. This means that of all the internal volume of the vehicle, only 85% of it could be effectively used for tanks and payload.

3.3.1 Rocket Vehicle System Element

The "Rocket" system element, shown in Figure 14, contains all the components to build a rocket. "RocketFuselage" specifies the physical parameters for rocket cylindrical length, diameter, ogive length and geometry. The user must make sure that the volume of the vehicle is enough to hold the volume of the vehicle's necessary components. This can be checked in the model's outputs after a convergence is complete. "Wing" defines the shape, position, weight characteristics, aerodynamic characteristics and sizing weight. In this study, all vehicle wings are sized off the vehicle's landing weight. For horizontal takeoff configurations, not included in this study, the wings would be sized from the GTOM. This study used a NACA Series 2412 airfoil sized for a landing speed of 185 knots. "Base", "ThrustStructure" and "AftSkirt" define the aft part of the rocket where the engines interface with the rest of the rocket structure.

"EngineCluster" is where the user defines the parameters for engine performance including area ratio, design altitude, and engine thrust-to-weight (T/W). This SysEl sizes

the fuel pump assembly, combustion chamber, and nozzle size. HySIDE includes preset parameters for a variety of existing engines or a user can specify a custom engine type. For this study, SSMEs and RD-180s (specifications are shown in Table 2) were scaled and used. SSMEs have a long history of use with shuttle and are considered the current standard in hydrogen fueled rockets. The RD-180, which has powered some of the Atlas series launch vehicles, is the industry standard in hydrocarbon fuel rockets [30]. One model, a tri-propellant, uses a RD-701 engine that runs on both hydrocarbon and hydrogen fuel. A vehicle thrust-to-weight ratio of 1.4 was used at takeoff because all vehicles takeoff in a vertical configuration.

Table 2. Rocket Engine Baseline Parameters

Engine	SSME	RD-180	RD-701
Fuel	LH_2	RP-1	RP-1/LH_2
Oxidizer	LOX	LOX	LOX
Mixture Ratio	6	2.72	3-6
T/W (engine)	73.12	78.44	111.22
Nozzle Area Ratio	77.5	36.87	133.8
Chamber Pressure (psia)	2,960	3,727	4,264
Characteristic Velocity (fps)	7,592	5,916	6,246
I_{sp} - SL (s)	363	311	330
I_{sp} - Vacuum (s)	453	338	415
Average Thrust - SL (lbf)	418,076	863,987	715,591
Average Thrust - Vacuum (lbf)	512,115	933,407	899,910
Weight (lbf)	7,004	11,890	8,091
Length (ft)	13.91	11.68	18.7
Diameter (ft)	5.35	9.84	7.55

"TankStack" outlines the volume-to-mass ratios for the propellant tanks and their relative locations within the rocket. This SysEl calculates the size and weight of the fuel and oxidizer tanks based on the required propellant volume produce by "Propellant-Usage" (discussed later). "StructuralWeightsFromVol" contains vehicle components who's mass is proportional to the volume of the vehicle. These include structural provisions, engine considerations, payload bay components and other miscellaneous

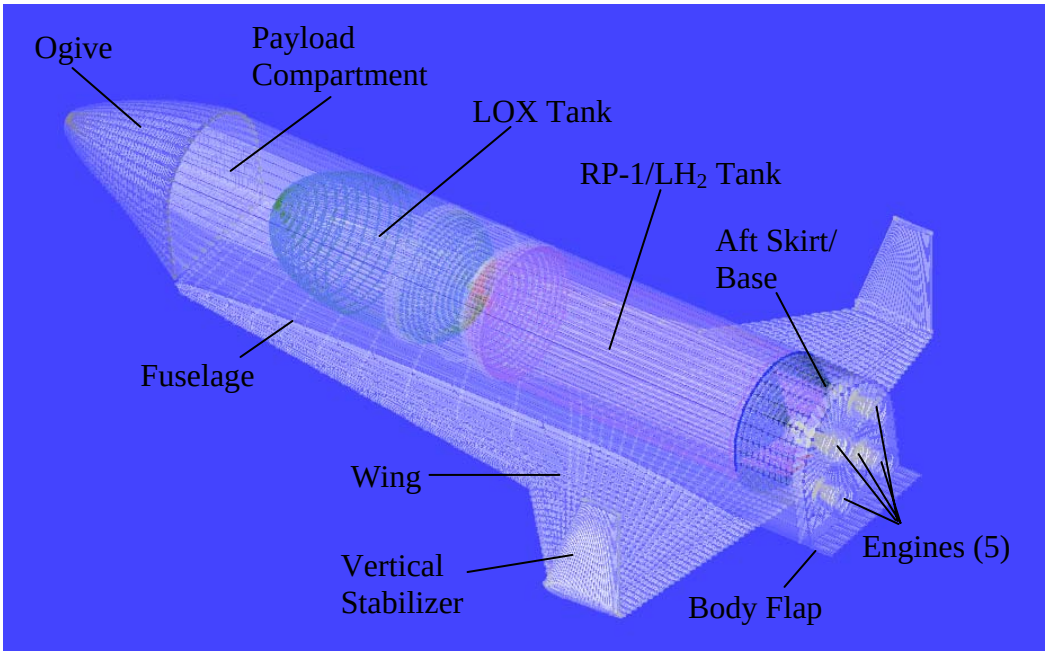

Figure 15. HySIDE Rocket Vehicle Model

items. The "StructuralWeightsFromWt" SysEl specifies trends for vehicle component masses that are proportional to the mass of the vehicle such as landing gear, reaction control system (RCS), OMS module and fly back propulsion (if needed). These two SysEls use historical trend curves to size components. An entirely assembled rocket vehicle is shown in Figure 15.

3.3.2 Hypersonic Airbreathing Design Optimization (HADO) Vehicle System Element

A RBCC model is built using a Hypersonic Airbreathing Design Optimization (HADO) SysEl called "HADOVehicleBasic". In the same way that the "Rocket" SysEl specified the physical characteristics of a rocket vehicle, "HADOVehicleBasic" contains all the modules that define the size and shape of an RBCC vehicle. The SysEl "Inlet" outlines the parameters for vehicle's inlet. The user defines the shape of the inlet as well as its size. "VehCapArea" is the measure of the cross sectional area of the vehicle inlet.

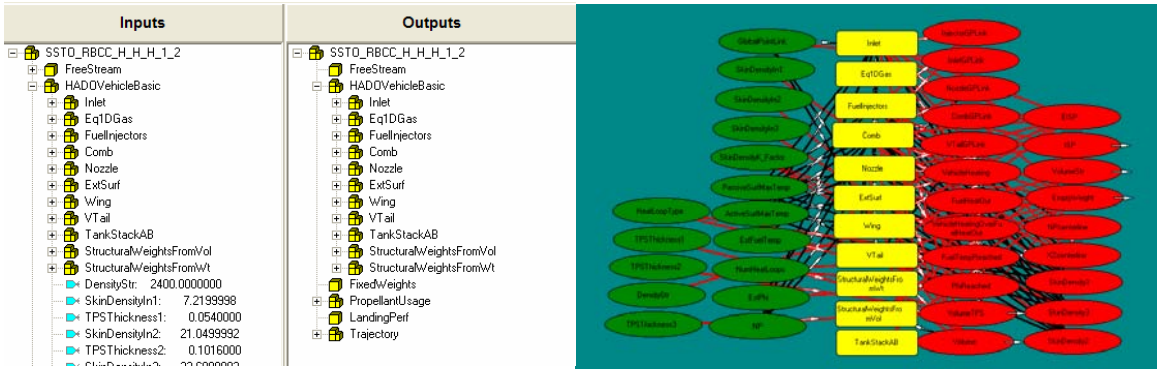

Figure 16. HADO System Element and I/O

This parameter is the means by which the user controls the physical size of the vehicle. Like "RocketFuselage", this value must be manual converged to make sure the volume ratio is greater than one. Further discussion about the inlet can be found in section 3.4.2. There are SysEls to size the fuel injectors and combustor as well. Once these parameters have been defined, the "ExtSurf" SysEl closes the surface by creating the rest of the fuselage to connect all the components. The "Wing" SysEl is used here to specify the size, shape and inputs for the wing in the same way as for a rocket. For all the VTHL models in this study, the landing mass was used to size the required wing area. For HADOs, there is a separate SysEl for the sizing of the vertical tail. "VTail" uses the size of the wings, along with a K-factor, to determine the required size of the tail for yaw stability. The user can also specify the sweep, taper ratio and airfoil type for the tail.

"TankStackAB" calculates the size and mass of the propellant tanks for RBCC vehicle. Compared to cylindrical tanks used in rockets, tanks used in these type of vehicles are conformal in shape and therefore have a larger mass per volume of propellant contained. There is a great deal of uncertainty in the trends of conformal tanks such as these. The SysEl uses the method of calculating rocket tank size and then applies a K-factor to account for the change in tank shape. To conform to previous studies, a K-

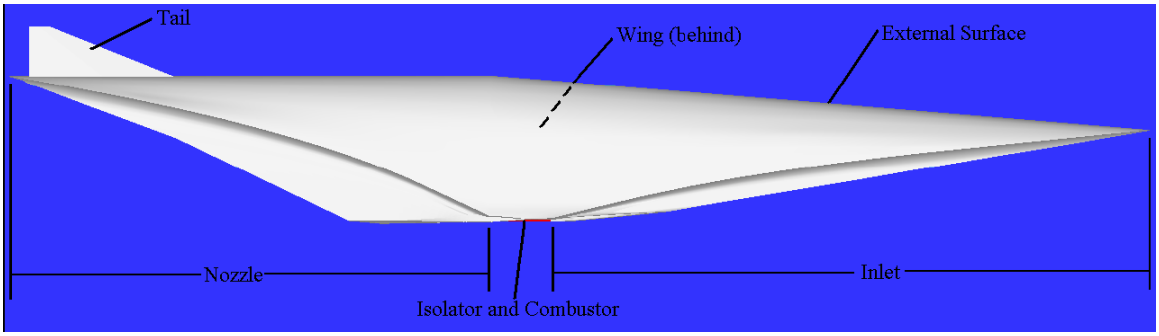

Figure 17. Cross Section of HySIDE RBCC Vehicle Model

factor of 1.4 was used for these tanks. Unlike the rocket tanks, the propellant tanks in airbreathing vehicles are not placed within the vehicle. Instead, their mass and volume are cataloged in a manner much like that used with "StructuralWeightsFromWt" and "StructuralWeightsFromVol" SysEls.

3.3.3 Common System Elements

Every type of RLV model uses a set of common SysEls that are independent of the vehicle type. The first is the "FreeStream" SysEl and specifies the design Mach number and altitude for the vehicle. For rockets, these parameters have minimal effect on the shape of the vehicle. For airbreathers however, these two parameters specify the optimal dynamic pressure for the inlet and nozzle. In the "Trajectoy" SysEl, the user can specify if the vehicle flies a constant-q profile while using the DMSJ. "FixedWeights" is where the user defines the non-scalling components of the vehicle. These include the size of the crew cabin (if manned), mass of the payload, volume of the payload, and room for future additions. This study used a 9,071.8 kg (20,000 lbm) payload module with a volume of 79.3 m^3 (2800 ft^3).

"PropellantUsage" contains the parameters that define the use of the vehicle's propulsion through the different stages of flight. The vehicle's ascent is broken into three separate stages whose boundaries are user-defined by four transition velocities. For

rockets, only the first and third stages are used. Airbreathers, however, use all three segments including the second scram-ramjet segment. The user also specifies the relationships between the vehicle velocity and I_{sp} for each segment of flight. These look-up tables can be selected from a menu of pre-sets or user customized. "PropellantUsage" has a module, "PropTypeDetails", were the user specifies which fuel and oxidizer are used on each segment. The propellant storage density, max tank pressure and mixture ratios are defined here. This SysEl tracks the mass flow of all propellants during flight and provides that data to the "TankSizing" module.

The "Trajectory" SysEl is the module that "flies" the modeled vehicle through its ascent. Using the vehicle's size and characteristics, defined by the other SysEls, "Trajectory" computes the forces acting on the vehicle using Missile DATCOM [11]. The user specifies the velocity versus altitude trajectory for each segment of flight. For the second segment, the user can constrain the trajectory to a constant dynamic pressure specified from the "FreeStream" SysEl. The position, velocity and acceleration are tabulated for every point along the vehicle's trajectory. At the end of each iteration, HySIDE compares the estimated GTOM with the required mass and adjusts the next iteration's guess as necessary until convergence is reached.

3.4 Design Assumptions

Each vehicle concept in this study was analyzed using a computational model to represent the real-world capabilities of the vehicle. These models are approximations and their accuracy is highly dependent on the assumptions that were used to generate them.

The following discusses the assumptions used in modeling the propulsion systems, ascent trajectory, airbreathing vehicle shape and propellant tanks.

3.4.1 Propulsion Systems

For each of the propulsion types modeled, assumptions were made to accurately predict the thrust, propellant usage and mass properties of each engine. HySIDE uses a "rubberized" engine sizing method which takes the known characteristics of a real engine, and scales the engine size to meet the needs of the model. Presented here is the data for the nominal engines to be scaled for the vehicle models.

3.4.1.1 DMSJ Engines

AFRL/PR has predicted the performance for a hydrocarbon DMSJ engine and this data was incorporated into this study. The predicted velocity versus I_{sp} values were tabulated and input into the HySIDE model as shown in Table 3. The full set of AFRL's I_{sp} data can be found in Appendix B [11]. For hydrogen fuel DMSJs, HySIDE's default

Table 3. HySIDE Hydrocarbon DMSJ Velocity vs. I_{sp}

V, ft/sec	ISP (sec)
0.000	0.000
3500.000	0.000
3750.000	1765.000
4000.000	1628.000
4500.000	1646.000
5000.000	1413.000
6000.000	975.000
7000.000	859.000
8000.000	771.000
8250.000	747.000
8500.000	650.000
9000.000	500.000
11000.000	100.000
13000.000	0.000

values were used (shown in Table 4). A tri-propellant DMSJ was analyzed in this study. The concept involves running the engine with hydrocarbon fuel until the fuel's thermal limits and then slowly transition to hydrogen fuel. This process allows the DMSJ to burn the high density hydrocarbon fuel and use the scramjet to higher Mach numbers. The data for all three fuel options is plotted in Figure 18.

Table 4. HySIDE Hydrogen DMSJ Velocity vs. I_{sp}

V, ft/sec	ISP (sec)
0.000	0.000
1000.000	85.000
2000.000	1000.000
2500.000	1600.000
3000.000	3000.000
4000.000	4880.000
4200.000	4922.000
4400.000	4700.000
4600.000	4444.000
4800.000	4193.000
5000.000	3971.000
7000.000	2808.000
10000.000	1734.000
17000.000	700.000
27000.000	0.000

Methods originally derived in the 2006 AFIT Study were used to determine the proper cutoff velocities for the DMSJ [11]. As the speed of the scramjet vehicle increases, the specific impulse of the DMSJ engine slowly tapers off (shown in Figure 18 with dashed lines). This trend continues until the temperature in the combustion chamber reaches the levels of material failure. At this point, then engine must add extra cold fuel into the engine, or "phi dump", to keep the engine temperatures within tolerance. This significantly reduces the specific impulse of the engine and is represented by solid lines

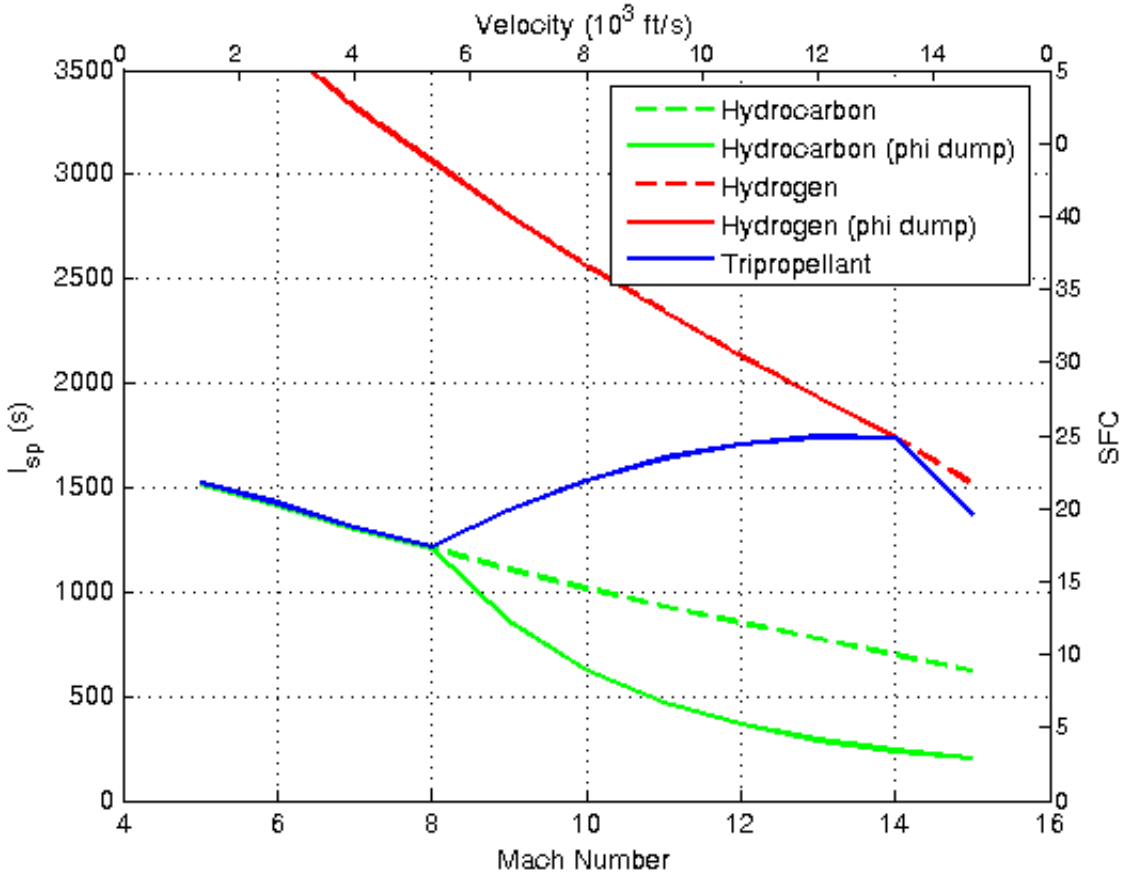

Figure 18. DMSJ I_{sp} vs. Mach Number for Different Fuels

in Figure 18. Determining the right time to switch to rocket propulsion involves the effective specific impulse as well as the fuel combination bulk density (shown in Table 5). For hydrogen DMSJ to hydrogen rocket, the cutoff velocity was 4,724 m/s (15,500 ft/s). For hydrogen DMSJ to hydrocarbon rocket, the cutoff velocity was 3,962 m/s (13,000 ft/s). For hydrocarbon DMSJ to hydrogen rocket, the cutoff velocity was 2,530 m/s (8,300 ft/s). For hydrocarbon DMSJ to hydrocarbon rocket, the cutoff velocity was 2,438 m/s (8,000 ft/s).

Table 5. Bulk Density for Different Propellant Combinations

Propellant	Bulk Density (kg/L)	Bulk Density (lb/ft^3)
RP-1/LOX	1.03	64.30
JP-7	0.82	51.19
LH_2/LOX	0.32	19.98
LH_2	0.07	4.37

3.4.1.2 Rocket Engines

Two techniques were used to increase the efficiency of rocket engines in this study. The first was the use of two-position nozzles to increase the efficiency of exhaust expansion through a wide range of altitudes. Conventional nozzle designs optimize the expansion, dominated by the nozzle's throat-to-exit area ratio, for an altitude mid-way though the ascent. This makes the exhaust over-expanded during the first phase of flight and under-expanded during the last phase of flight. Two-position nozzles have two separate nozzle components that make the nozzle structure. This allows the nozzle to be optimized for two altitudes in the rocket's ascent. At low altitudes, the second part of the nozzle is tucked away. When the larger area ratio becomes more optimal, it moves into position and increases the area ratio of the engine. While this system increases the overall specific impulse of the engine, the extra equipment is a weight penalty to the engine. An optimization was performed to find the two best area ratios for both SSME and RD-180 engines. Plots of these engine's specific impulses are provided in Appendix C.

The second technique employed in this study was the use of tri-propellant rockets. Three different configurations were used to implement tri-propellant rocket propulsion. The first uses two separate engines, one burning hydrogen and one burning hydrocarbon, used in tandem. Both engines are sized for the initial weight of the vehicle. Both engines burn during the initial phase of flight and only the hydrogen engine burns at the end of a vehicle's ascent. The second method is to use two separate engines that burn at different times. The hydrocarbon engine is sized for takeoff and burns during the initial phase of flight until the hydrogen engine takes over and propels the vehicle during the final phase

of flight. The last method uses one engine type that burns both hydrogen and hydrocarbon in the same flow path. An experimental engine that uses this technique is the RD-701 [30]. An optimization was conducted to find the ideal velocity to switch between propulsion fuels.

3.4.2 Inlet and Nozzle Assumptions

In a RBCC vehicle, the external surface of the vehicle acts as both the engine's compressor and nozzle. HySIDE uses four SysEls to define the engine inlet: "RDP", "RcH", "LH" and "VelCapArea". The Radial Deviation Parameter (RDP) specifies the shape of the inlet and varies from 1 to -1. A RDP of -1 generates a "spike" shape with the nose of the vehicle at the center of the flow field. A value of 1 produces an inward-turning, or bowl, shape that places the inlet around the compressing flow field. A RDP of 0 correlates to a flat, or 2-D, inlet with no lateral curvature. Previous studies have shown that inward-turning inlet shapes have higher performance and therefore were the only inlets considered in this study [7]. Appendix A shows the inlet shape associated with varying RDP. In addition to the curvature of the inlet, "RcH" and "LH" further define the shape of the inlet cross section. "RcH" specifies the sweep of the inlet leading edge. No sweep would be a blunt edge while larger values make the leading edge sharper. In a 2-D inlet, "LH" is a height-to-width ratio. In turning inlets, this variable corresponds to the amount of arc an inlet occupies. For inward turning inlets, a value of π makes a semi-circle and a value of 2π results in a closed inlet.

With the points of the inlet leading edge defined, HySIDE uses isentropic shock relations and inviscid flow to produce streamlines flowing into the engine. The method

of characteristics is used to define the surface geometry to produce the desired compressive flow. This defines the outer mold-lines of the compressor. From the final inlet geometry, aerodynamic and thermodynamic properties can be calculated. The weight of the inlet accounts for which sections require actively- and passively-cooled temperature regulation.

The exhaust nozzle is determined in the same fashion as the inlet. The flow exiting the combustor is used as the input to the nozzle and a method of characteristics determines the mold-line that produces the desired flow field shape. The user can specify a truncation factor to end the nozzle before the flow is fully expanded.

3.4.3 Trajectory Assumptions

Rocket and airbreathing SSTO vehicles differ greatly in their trajectories to orbit. All rocket models follow an optimized 'direct ascent' trajectory to orbit. These trajectories spend the least amount of time in the Earth's thick atmosphere. RBCC vehicles have a 'constant q' segment between rocket segments. During this DMSJ

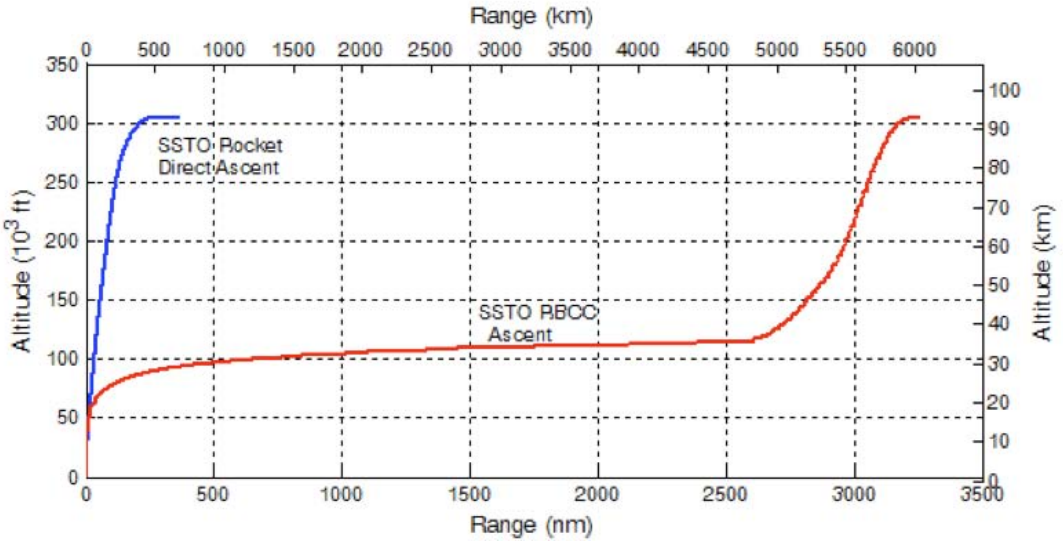

Figure 19. Rocket and RBCC Ascent Trajectories

trajectory portion, the vehicle is gaining altitude to decrease density and maintain a constant dynamic pressure as the speed of the vehicle increases. This keeps the DMSJ operating at peak performance. This segment takes a lot of time and makes the time of flight (TOF) of SSTO RBCC RLVs significantly longer than that of rockets.

3.5 Mission Description

Each RLV is tasked with vertically launching a 9,071.8 kg (20,000 lbm) payload module with a volume of 79.3 m^3 (2800 ft^3). The launch point is assumed to be Kennedy Space Center (Latitude=28.6° N) and the point of MECO is an elliptical orbit of 50 nm or 92.6 km (303,800 ft) perigee and 100 nm or 185.2 km (607,612 ft) apogee. Orbital velocity at MECO is 7,468.5 m/s (24,503 fps) and the orbital inclination is 28.6°. Once at apogee, the OMS circularizes the orbit. The OMS is sized for a total ΔV of 240 m/s (787.4 ft/s). Once in orbit, the payload module is deployed in whatever fashion is appropriate to the mission. The payload may be a LEO satellite or a satellite with its own propulsion to take it to a higher orbit. Once the payload is released, the RLV executes an OMS de-orbit burn, re-enters the atmosphere and lands. The vehicle will then undergo maintenance, payload integration and then re-positioned for the next launch.

4. Results and Analysis

This chapter overviews and discusses the results obtained in this study. Astrox Corporation's HySIDE code was used to model each vehicle and produce vehicle performance outputs. Vehicles were sized to be reusable and lift a 9,071.8 kg (20,000 lbm) payload module with a volume of 79.3 m^3 (2800 ft^3) into a 100 nm circular orbit. Rocket and airbreathing engine performance characteristics were modeled after near-term state-of-the-art capabilities based off current research. With the exception of unique engine and fuel options, all input parameters were kept the same between vehicle configurations. A detailed list of model inputs is provided in Appendix D for reference. By using this consistent analysis method, vehicle configurations could be compared on an 'apples-to-apples' basis.

The first section of this chapter presents the sized vehicle outputs from HySIDE. The second section discusses empty mass trends between different vehicle types. The third section discusses the trends associated with vehicle empty, payload and propellant mass fractions. The forth section discusses trends in the exposed, or wetted, area of each vehicle. The fifth section compares these results with those of previous studies using HySIDE. Finally, this chapter concludes with a summary of results obtained.

The model configurations in this study are labeled in three or four parts: Two- or single-stage, propulsion type, fuel type and engine configuration (if applicable). Number of stages in a vehicle model are denoted by a "SSTO" or "TSTO". Vehicles labeled with "Rkt" use rocket propulsion while vehicles labeled with "RBCC" use rocket-based combined-cycle DMSJ propulsion. Hydrogen fuel vehicles are labeled with an "H" and

Hydrocarbon fuel vehicles are labeled with "HC". For SSTO RBCC vehicles, the three fuel symbols describe the fuels used on each of the three stages of ascent. In the three tri-propellant SSTO rocket configurations, "2T" denotes separate hydrogen and hydrocarbon engines that burn in tandem, while "2S" represents separate engines that burn in series and "1S" symbolizes one engine type that first burns hydrocarbon and then hydrogen.

4.1 HySIDE Model Outputs

In this study, empty weight and wetted area were the primary figures of merit when comparing vehicle configurations. Table 6 lists the 16 vehicle models (and one model that did not converge) and their sizing characteristics. The SSTO RBCC H-H-HC vehicle model failed to close. This configuration represents an inefficient design by placing the hydrogen burn at the beginning of the ascent and hydrocarbon at the end. Hydrocarbon fuels, with their large bulk densities, are best when used during the initial

Table 6. RLV HySIDE Outputs

Vehicle	GTOM (kg)	GTOW (lbs)	Empty Mass (kg)	Empty Weight (lbs)	Empty Mass Fraction	Payload Mass Fraction	Propellant Mass Fraction	Wetted Area (m^2)	Wetted Area (ft^2)
TSTO Rkt H	567,089	1,250,204	99,540	219,446	17.55%	1.60%	80.85%	2,566	27,624
TSTO Rkt HC	661,834	1,459,080	86,822	191,408	13.12%	1.37%	85.51%	1,814	19,527
SSTO Rkt H	1,320,538	2,911,258	174,387	384,455	13.21%	0.69%	86.10%	3,989	42,936
SSTO Rkt HC	2,709,250	5,972,812	202,748	446,978	7.48%	0.30%	92.22%	3,922	42,214
SSTO Rkt HC/H 2T	1,312,137	2,892,737	160,677	354,228	12.27%	0.69%	87.04%	3,418	36,787
SSTO Rkt HC/H 2S	1,247,459	2,750,148	152,276	335,707	12.21%	0.73%	87.06%	3,278	35,283
SSTO Rkt HC/H 1S	1,102,611	2,430,816	120,640	265,962	10.94%	0.82%	88.24%	2,948	31,734
TSTO Rkt H / RBCC H	265,027	584,278	72,366	159,539	27.31%	3.42%	69.27%	2,102	22,626
TSTO Rkt HC / RBCC H	286,723	632,109	61,431	135,430	22.57%	3.33%	74.10%	1,717	18,483
TSTO Rkt HC / RBCC HC	343,598	757,497	46,036	101,492	13.40%	2.64%	83.96%	1,183	12,736
SSTO RBCC H-H-H	571,436	1,259,787	137,288	302,666	24.03%	1.59%	74.38%	3,182	34,254
SSTO RBCC HC-H-H	481,360	1,061,206	102,673	226,353	21.02%	1.86%	77.12%	2,459	26,472
SSTO RBCC H-H-HC	*no covergance*								
SSTO RBCC HC-H-HC	1,193,883	2,632,034	180,068	396,978	15.08%	0.76%	84.16%	3,345	36,005
SSTO RBCC HC-HC/H-H	600,448	1,323,748	67,396	148,581	11.22%	1.51%	87.26%	2,337	25,154
SSTO RBCC HC-HC-H	555,971	1,225,693	84,784	186,914	15.03%	1.61%	83.36%	1,847	19,878
SSTO RBCC HC-HC-HC	943,285	2,079,566	107,776	237,602	11.25%	0.95%	87.80%	1,853	19,944

portions of the ascent while hydrogen fuels, providing high I_{sp} performance, are best when used at the end of a vehicle's ascent. This trend is discussed further in following sections.

4.2 Empty Mass Trends

The gross takeoff mass and empty mass are plotted for all vehicles in this study in Figure 20. Gross mass does not indicate where mass is allocated (structure, payload or mass) and consists of mostly inexpensive propellant. It is presented here for reference. Empty mass is a good indication of procurement and operational costs because it consists of the expensive structure of the vehicle. The area in green represents the region of vehicles with an empty mass of less than 11,340 kg (25,000 lb). This is an arbitrarily-

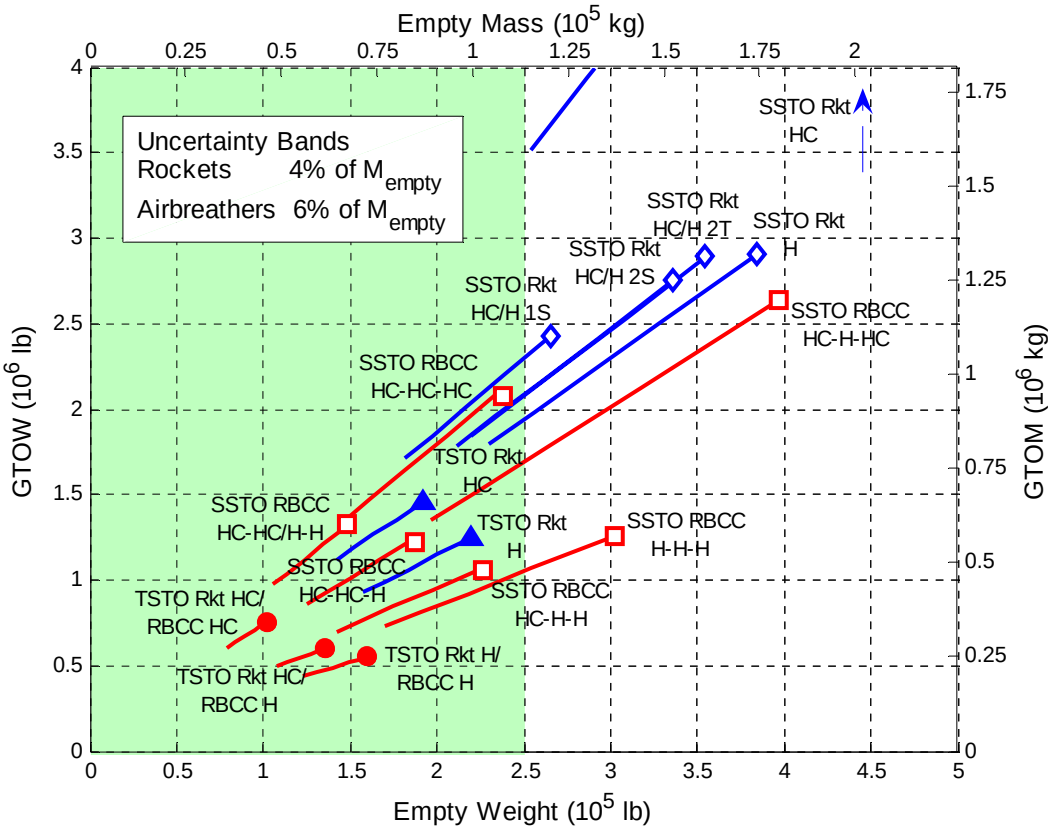

Figure 20. RLV Empty Mass vs. GTOM

chosen region representing the limits of a vehicle that can be practically procured and operated given the current economic and political environment.

In Figure 20 there are distinct groupings of vehicle types. In general, airbreathing vehicles tend to reduce the empty weight of a vehicle when compared to rockets. The lightest group of vehicles is the TSTO Rkt-RBCCs. Among these vehicles, the all-hydrocarbon fuel configuration has the lowest empty mass but the largest GTOM. This trend can be found in other vehicle types as well. Hydrocarbon fuel vehicles have smaller empty masses than their hydrogen fuel counterparts. This is due to the higher density of hydrocarbons, resulting in a smaller vehicle volume causing a reduction in the structural mass needed to support the vehicle. Conversely, the low energy-per-mass of hydrocarbons means that more propellant mass is required giving hydrocarbon vehicles higher gross, or fueled, mass. The second smallest grouping is the TSTO rockets. These systems represent the highly conventional vehicles that are capable of use today. Like the Rkt-RBCC group, the all-rocket hydrocarbon vehicle has a larger GTOM and lower empty mass than the all-hydrogen rocket.

The most massive type of vehicles by far is the SSTO rockets. The largest vehicle in this group is the hydrocarbon rocket. This vehicle is heavier in empty weight than the hydrogen SSTO rocket. This switch in behavior is a result of the large structural mass of a SSTO vehicle pared with the low I_{sp} performance of hydrocarbon fuel rockets. The large empty weight and bulk density of hydrocarbon fuel give this vehicle a very large GTOM (not shown in figure). Of the three tri-propellant SSTO rockets, the vehicle that burns both fuels in one engine was the lightest. Compared with the other two tri-propellant rockets, this configuration has the greatest engine thrust-to-weight ratio. The

other two tri-propellant vehicles use separate engines for burning each fuel, thus reducing the overall engine thrust-to-weight.

The last group of vehicles is the most widespread and also the most interesting. The SSTO RBCC vehicles vary in size from the region of SSTO rockets down to TSTO rockets. The all hydrogen vehicle is a good starting point for consideration. Its empty weight is just outside the bounds of practicality and is 38% heavier than the hydrogen TSTO rocket. Using hydrocarbon in the first boost-segment reduces the empty weight to that of TSTO rockets. Switching to a hydrocarbon DMSJ further reduces the empty weight to match the hydrocarbon rockets. By using a tri-propellant DMSJ, the empty weight is reduced even further, beating the TSTO rockets by 22.4%. This is the lightest SSTO configuration in empty mass. Using hydrocarbon on all three stages increases both the empty and gross mass, but the empty mass remains on par with the TSTO rockets. Finally, using a hydrocarbon boosted, hydrogen DMSJ and hydrocarbon boost RBCC significantly increases the size of the vehicle. This is by far the largest SSTO RBCC and represents an inefficient configuration. During the last segment of flight, this vehicle is pushing a hydrogen-sized structure with a hydrocarbon I_{sp}. This vehicle (along with the non-converging H-H-HC vehicle) incorporates the worst elements of both fuel types.

The trend lines in Figure 20 show the weight sensitivity to vehicle size uncertainty. Monte Carlo simulations show that the uncertainty in the empty weight fraction of rockets is near 4% [18]. For airbreathing vehicles however, the uncertainty is much greater. This study assumed the uncertainty was approximately near 6%. The trend lines show the effect of these uncertainties on the vehicle masses. The length of the line represents how sensitive the vehicle design is to changes in empty mass. Vehicles

with long lines have higher growth factors and are more difficult to close. Short lines dictate that a design is stable. The trend lines are all in the direction of lighter empty weights with the data points at the most conservative end. Future technology improvements will drive the designs to be smaller and less massive. The most sensitive SSTO vehicles are the rockets and the least sensitive are the RBCCs. The relationship between payload mass, empty mass fraction, propellant mass fraction and GTOM is given by

$$m_{gross} = \frac{m_{payload}}{1 - f_{empty} - f_{propellant}} \tag{12}$$

where f_{empty} and $f_{propellant}$ are the empty and propellant mass fractions. m_{gross} and $m_{payload}$ are the gross and payload masses.

4.3 Empty Mass Fraction Trends

In Figure 21, the empty mass fraction is plotted against the vehicle empty mass. The shaded region again represents the limits of vehicle practicality. Notice that vehicles with hydrogen fuel have larger empty mass fractions than those with hydrocarbon fuel. This is a direct result of the density difference between the two fuels. Rockets in large have smaller empty weight fractions than airbreathing vehicles. This is due to the nature of the two propulsion types. Airbreathing vehicles require less propellant mass fraction and a more complicated structure (thus more massive) than rockets.

The two parameters that have the most effect on the mass sensitivity to empty mass fraction uncertainty are empty mass and empty mass fraction. Vehicles in the bottom-left corner of Figure 21 have the least sensitivity while vehicles towards the top

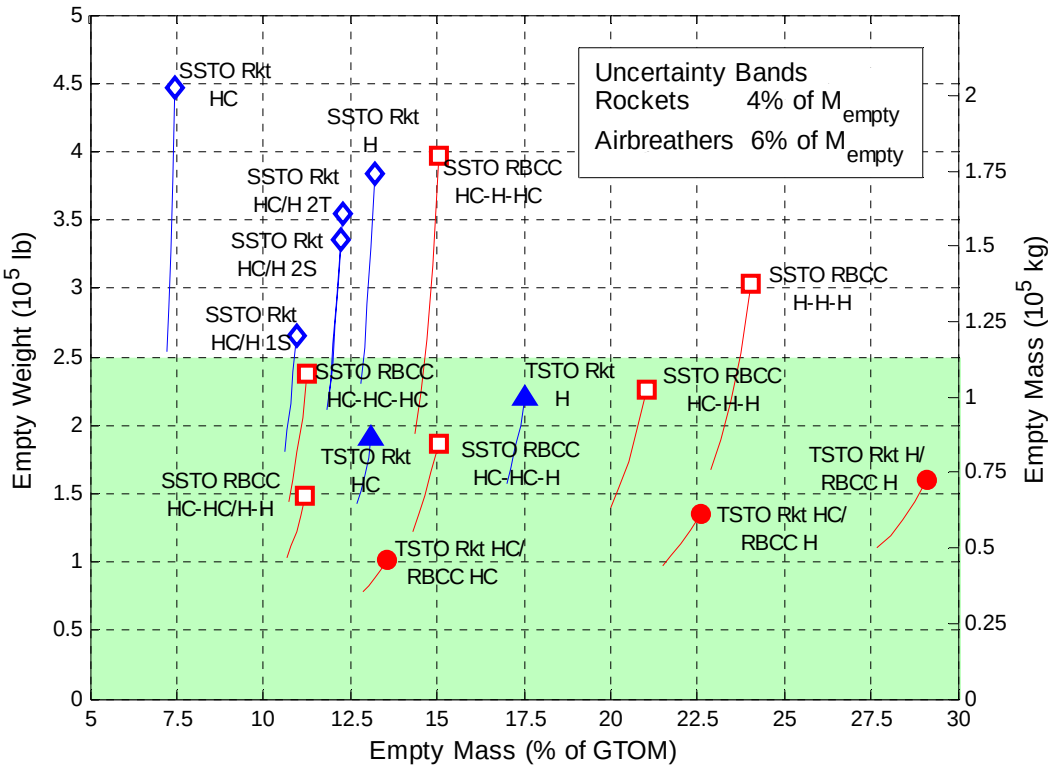

Figure 21. RLV Empty Mass Fraction vs. Empty Mass

or right have the most. The SSTO with the least sensitivity is the hydrocarbon boosted, tri-propellant DMSJ, hydrogen boosted RBCC. The vehicle that is most sensitive to empty mass fraction uncertainty is the inefficient HC-H-HC RBCC.

4.4 Wetted Area Trends

Figure 22 plots vehicle empty mass vs. wetted area. Wetted area, or the amount of external surface exposed to the external environment, is an excellent figure of merit for the cost of maintenance. The amount of the TPS required on a vehicle is roughly linear to the wetted area. Time of flight has a secondary effect on TPS requirements and is presented in Appendix E. There is a non-linear relationship between the wetted area and mass of a vehicle. Based on a theoretical, spherical body, this relationship is

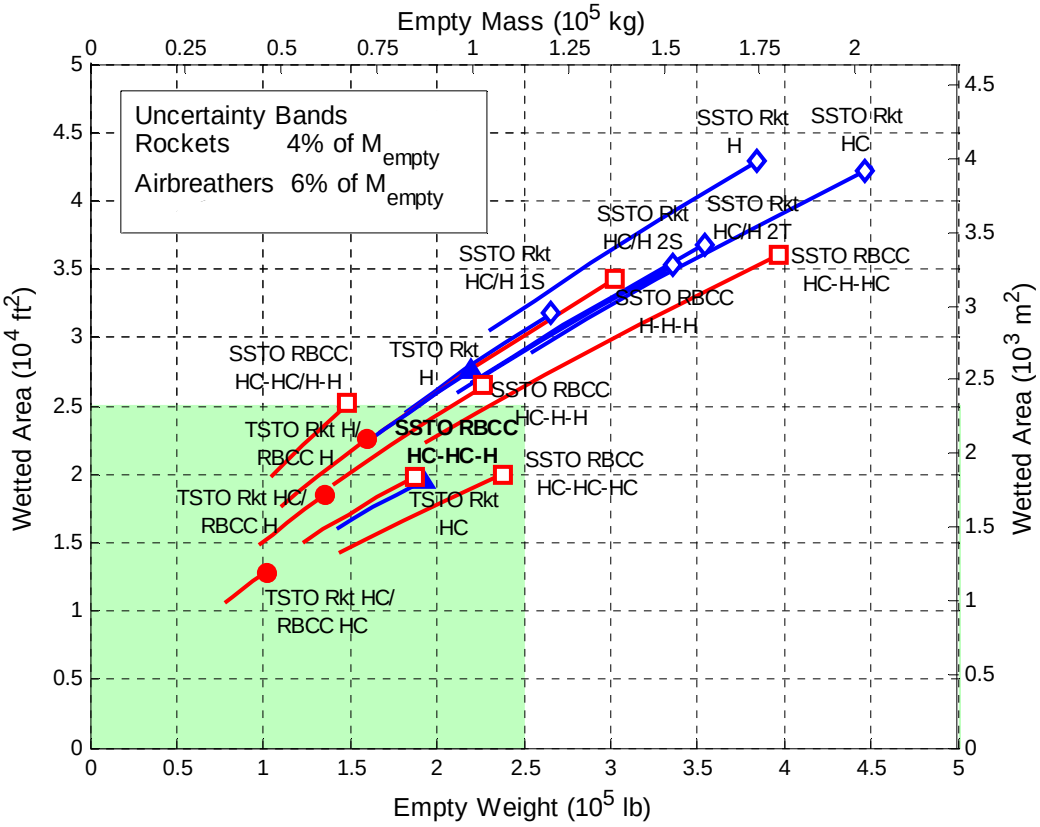

Figure 22. RLV Empty Weight vs. Wetted Area

$$A_{wetted} = (4\pi)\left(\frac{3m}{4\pi\rho}\right)^{2/3} \qquad (13)$$

where ρ is the effective density of the vehicle and does not vary significantly with vehicle size for a given design. In addition to the 11,340 kg (25,000 lb) empty mass cut-off, a wetted area limit of 2,323 m^2 (25,000 ft^2) was imposed as the practical limit for procurement.

Just as in the GTOM graph, Figure 22 shows the vehicles breaking into groups. Again, the TSTO rocket-RBCC vehicles are the lightest and have the smallest wetted areas. The all hydrogen vehicle is the biggest of this group in both mass and wetted area. The all hydrocarbon vehicle is the smallest in both respects with the HC/H vehicle somewhere in the middle. The TSTO rockets are the next group and are slightly heavier

and larger than the rocket-RBCC vehicles. Both rocket-rocket systems have roughly the same empty mass but the hydrocarbon fuel vehicle has significantly less wetted area. The low wetted area of the hydrocarbon fuel vehicles in these two groups is a result of the higher bulk densities of hydrocarbon propulsion.

The SSTO rockets are the largest and most massive group of the study. The band of SSTO rockets is well outside the realm of practicality. The single-fuel rockets are roughly the same size with the hydrocarbon rocket being the more massive. The use of two engine types and tri-propellants moves the rockets down in both categories. The single engine type, tri-propellant rocket is the best SSTO rocket and almost reaches the band of TSTO rockets.

For the SSTO RBCC vehicles, the use of hydrocarbon decreases both the empty weight and wetted area of the vehicle. The all hydrogen vehicle is the largest and most massive (with the exception of the impractical HC-H-HC configuration) and lies far away from the TSTO rockets. Using hydrocarbon on the boost phase significantly reduces both the empty weight and wetted area and compares well with the TSTO hydrogen rocket. Further use of hydrocarbon, in the DMSJ, brings the mass and wetted area down further and is the same size as a TSTO hydrocarbon rocket. By switching to a tri-propellant DMSJ, the empty weight is further reduced but the wetted area increases. This is due to the decrease in the average density of the fuel being used during the ram-scramjet segment. The all-hydrocarbon RBCC has a larger empty weight than three of the other configurations. However, this increase in empty weight and change in fuel does not bring a noticeable penalty in wetted area. Along with the HC-HC-H configuration, the all-

hydrocarbon fuel RBCC has the smallest wetted area of all the SSTO RBCCs. For RBCCs, the use of hydrocarbon in the boost phase always decreases the wetted area.

The sensitivity lines show that TSTO vehicles are less sensitive to empty weight uncertainty than SSTO vehicles. All the SSTO rockets are very sensitive to empty mass uncertainty as well as the large SSTO RBCC vehicles. The smaller SSTO RBCC vehicles have only slightly larger sensitivities than those of the TSTO rockets.

4.5 Growth Factor Trends

Figure 23 plots the vehicle empty mass growth factor vs. vehicle empty mass. Growth factor is a measure of how much a vehicle's empty mass changes given an increase in payload mass. A growth factor of 10 would mean that adding one kilogram of

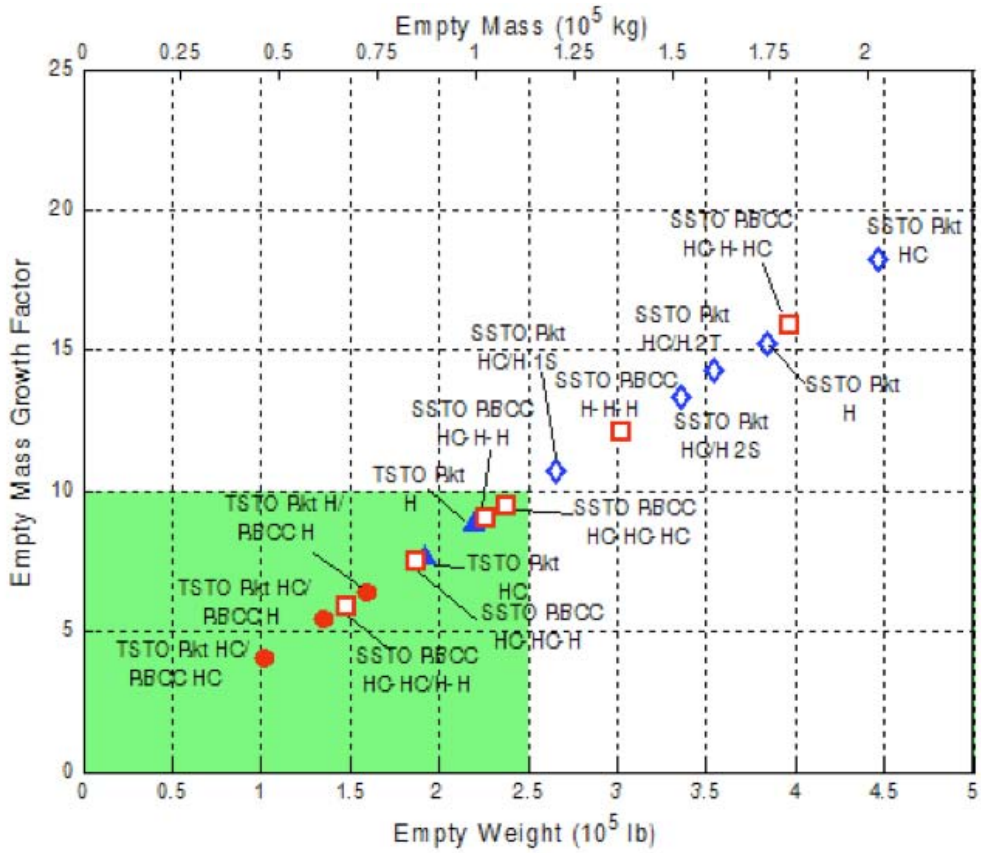

Figure 23. RLV Growth Factor vs. Empty Weight

payload would entail adding ten kilograms of vehicle empty mass to lift that mass into orbit. Vehicles that are highly sensitive to payload mass have high growth factors and are therefore not practical for operational use. The green region in Figure 23 bounds where practical vehicles exist. A growth factor over 10 was considered in this study to be too high for an operational RLV. Two stage systems have the lowest growth rates and all lie under the threshold of practicality. This is an inherent characteristic of the staging process. The four small SSTO RLVs had growth rates under 10 with the tri-propellant configuration having the best at just over 6. All the SSTO rockets had large growth factors that were over the practical threshold. The rocket with the smallest growth factor was the single-engine type, tri-propellant SSTO RLV. Among the SSTO RLVs, the airbreathers had much smaller growth factors, making them better candidates for an operational vehicle.

4.6 Time of Flight

The total time of ascent has secondary effects on how much TPS is required on an RLV. The longer a vehicle's wetted area is exposed to the heating due to atmospheric drag, the more TPS per area is required. This affects the maintenance cost of an RLV. Figure 24 plots the wetted area of each RLV with the time of flight (TOF). All the rockets had similar time of flights between 250 – 400 seconds. The similarity between rocket TOFs is because they share similar direct-ascent trajectories. Vehicles using DMSJ propulsion have higher TOFs because the vehicles accelerate slowly during the airbreathing portion of the ascent. The TSTO airbreathing RLVs had the second lowest TOFs because they are both two-stage and have airbreathing propulsion. SSTO RBCC

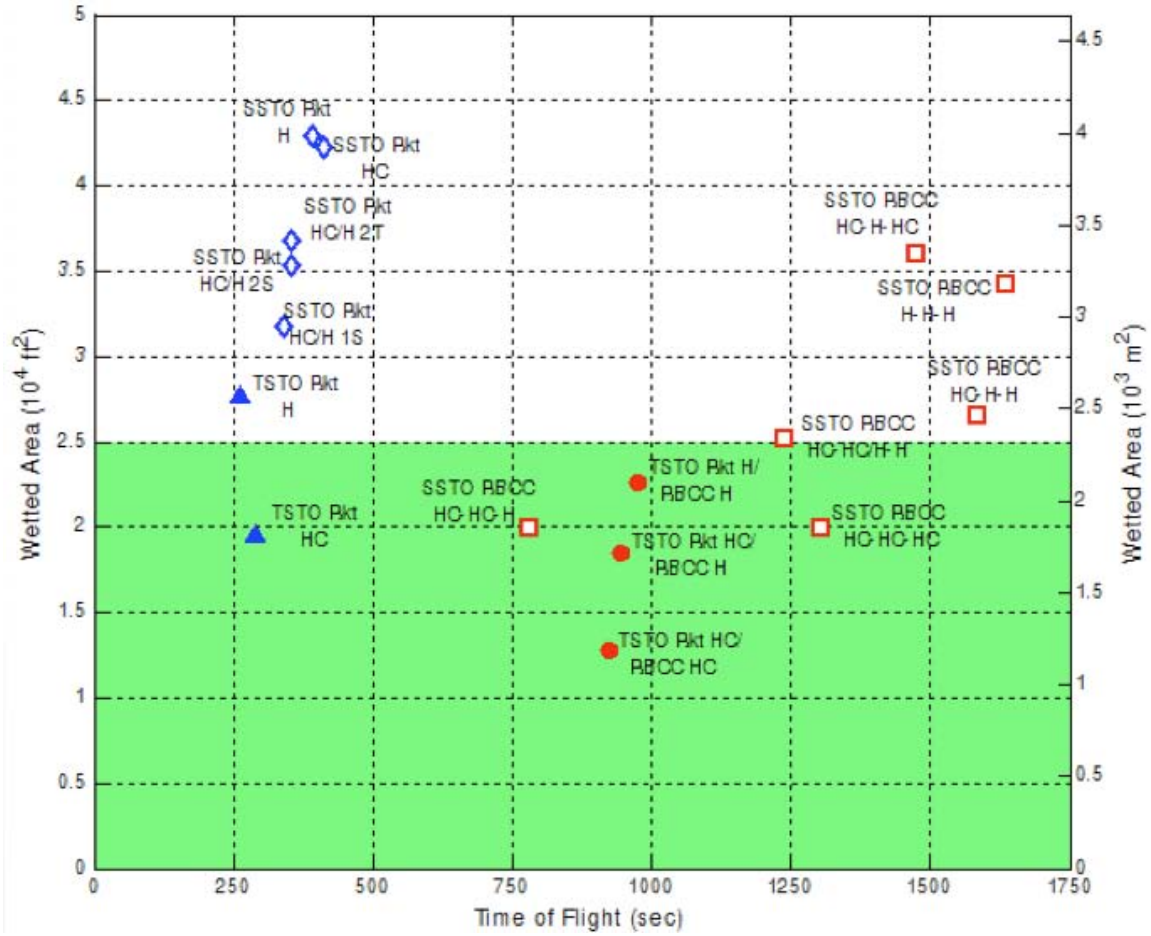

Figure 24. RLV Wetted Area vs. Time of Flight

RLVs had the largest TOFs. RBCCs that use hydrocarbon for the DMSJ had the lowest TOFs among SSTO RBCCs. This is due to the lower velocity range the DMSJ is used for. On these vehicles, rocket propulsion is used over a greater percentage of the ascent and decreases the TOF.

4.7 Rocket Nozzle Area Ratios

For the bi-propellant SSTO rockets, an optimization was performed to find the best two nozzle area ratios. The smaller nozzles were optimized for an altitude of 22.9 km (75,000 ft) and the larger nozzles were optimized for an altitude of 68.6 km (225,000 ft). For the hydrogen SSTO rocket, optimal area ratios were found to be 40 and

120. Area ratios for the hydrocarbon SSTO rocket were found to be 30 and 110. Data of specific impulse vs. altitude can be found in Appendix C.

4.8 Validation

The methods used in this study were based on those used in previous research efforts at AFIT using HySIDE to model RLVs. Model performance inputs were the same as those used in the 2006 AFIT study wherever appropriate [11]. There are three pertinent studies to compare to this study. The first is a study at the Lawrence Livermore National Lab in 1996 [25]. The study concluded that hydrogen and hydrocarbon fuel SSTO rockets should have propellant mass fractions roughly equivalent to 87% and 92% respectfully. In this study, the hydrogen SSTO rocket has a propellant mass fraction of 86.1% and the hydrocarbon SSTO rocket has a propellant mass fraction of 92.2%. These are in close agreement.

A 2004 study by the Aeronautical Systems Center (ASC) at Wright-Patterson AFB found sizing solutions for a wide range of RLVs including SSTO rockets and airbreathers [18]. The results of this study compare very well with the models in this study. However, the SSTO models in this study are all heavier and larger than those from the ASC study. The differences can be attributed to the assumptions made in both studies. This study chose to use conservative inputs when sizing vehicles, especially on airbreathing models. This was done to give a ‘worst case’ result for the vehicles. However, the trends between both studies are the same between vehicle configurations.

Another study by the Astrox Corporation in 2005 used HySIDE to model SSTO and TSTO vehicles [6]. Two configurations, hydrogen and hydrocarbon fuel SSTO

RBCCs, were analyzed in that study that compare to vehicles in this study. The hydrogen model in this study is on the high end of the uncertainty band for the Astrox model in both empty weight and wetted area. The hydrocarbon vehicle in this study is just beyond the uncertainty of the Astrox model in empty weight but within the uncertainty in wetted area. Again, these differences are attributed to different assumptions made by the researchers involved. While the vehicles in this study are larger than those from the Astrox study, the vehicle trends in empty weight and wetted area are the same. The results of this study can be seen as 'shifted' towards heavier empty weights.

The correlation between the results of this study and the results of previous research indicates that the methods used in this study are valid and the models are accurate. Do to assumptions made in this study, these SSTO results may represent the high-end of each vehicle's capabilities in regards to mass and size.

4.9 Summary

This study showed the results of different design configurations completing the same mission of launching a 9,071.8 kg (20,000 lbm) payload module with a volume of 79.3 m^3 (2800 ft^3) into orbit. This study found that hydrocarbon fuel vehicles tend to have smaller empty weights, smaller wetted areas but higher GTOMs than hydrogen fuel vehicles. In general, airbreathing vehicles had empty weight advantages over rocket vehicles. Additionally, vehicles with large empty mass fractions and empty masses were highly susceptible to changes in the empty mass. These vehicles' high sensitivities to mass uncertainty make them unlikely candidates for development due to lack of room for future additions and mass budget overshoots. The results demonstrated that there are

viable vehicle configurations that use mostly, if not all, hydrocarbon fuel. Of all the configurations considered, the hydrocarbon boosted, tri-propellant DMSJ, hydrogen boosted (HC-HC/H-H) RBCC was the lightest SSTO in empty weight and wetted area. The single-engine type, sequentially burned, tri-propellant (HC/H 1S) rocket was the smallest and lightest SSTO rocket considered.

5. Conclusions and Recommendations

This research effort endeavored to look at a variety of RLV designs and compare their performance. There has been a great deal of research in the use of hydrogen-fueled airbreathing launch vehicles, but little research has been conducted on the potential benefits of hydrocarbon-fueled scramjet engines. Hydrocarbon fuel has many benefits over hydrogen. It does not have the stringent requirements on cryogenic storage like hydrogen and can therefore be transported and stored more easily. These logistical concerns are critical for military space launch applications. Current research by the Air Force's HyTech program is focusing on the development of a hydrocarbon scramjet due to the practical benefits of this technology. The results of this study with hopefully give researchers and decision makers more insight into the potential of vehicles using hydrocarbon-airbreathing propulsion technology.

5.1 Conclusions of Research

1. In the realm of SSTO RLVs, rocket systems do not perform as well as airbreathing systems. They have high empty mass and propellant mass fractions which drive the empty weight to be greater than that of other vehicle types. SSTO rockets also had some of the highest wetted areas of the vehicle configurations considered meaning that they would require more TPS and maintenance man-hours than other vehicles with smaller wetted areas. The use of airbreathing technology reduces the empty weight of the system significantly. Some of the SSTO RBCC vehicles had empty weights comparable to that of TSTO rocket systems. TSTO rocket systems are the current standard in space

access. An SSTO vehicle with equal or lesser weight than the current standard in space launch is significant.

2. For SSTO rocket systems, the use of tri-propellants reduced both the empty weight and wetted area. Of the tri-propellants, the vehicle with the RD-701 engine preformed the best. This engine's high thrust-to-weight ratio and ability to burn both hydrocarbon and hydrogen fuel make it ideal for a SSTO rocket RLV. The other two tri-propellant SSTO rockets use two separate clusters of engines that each have their own pump assemblies, combustion chambers, and nozzles. This significant weight penalty drives these vehicles to be larger than the RD-701 design. In fact, these two designs are so close in size and mass to the all-hydrogen SSTO rocket that it would make no sense to use them.

3. Growth rates for SSTO vehicles are greater than those of TSTO vehicles. Additionally, the larger the empty weight of the vehicle, the larger the vehicle's growth rate. This behavior is a result of the relationship between vehicle weight and an ever-increasing empty weight fraction. From Equation 12, as the denominator approaches unity, the gross size of a vehicle asymptotically approaches very large numbers. For the heavier vehicle configurations, they are much closer to the design limits and are therefore more sensitive to changes in the vehicle's inert mass.

4. For airbreathing SSTO RLVs, the use of hydrocarbon fuel during the initial boost phase significantly reduces the empty weight and wetted area. This is caused by the reduction in tank size and mass for the first stage propellants. This reduction in mass and drag affect the last two stages of flight by decreasing the amount of vehicle that must be pushed thought the atmosphere and accelerated to orbit.

5. The use of a hydrocarbon fuel DMSJ on SSTO RBCC RLVs significantly reduces the wetted area of the vehicle. In the case of the HC-HC-H configuration, it also reduced the empty weight of the vehicle. Even though the hydrocarbon fuel DMSJ has a lower I_{sp} and can't perform over the range of speeds as a hydrogen DMSJ, the savings in vehicle mass overcompensate for this performance penalty.

5.2 Recommended SSTO Configurations

1. The best SSTO rocket RLV is the RD-701 powered, tri-propellant configuration. This vehicle had the smallest empty mass, gross takeoff mass, wetted area, and growth rate. This vehicle relies on current state-of-the-art propulsion technology and conventional vehicle fabrication technology and techniques. This system closely resembles what is currently being used for access to space. While it does not perform as well as some of the airbreathing RLVs, this system is not prone to the massive amount of uncertainty that lies in the potential of airbreathing technology.

2. The SSTO RLV with the lowest empty weight is the hydrocarbon boost, tri-propellant DMSJ, hydrogen boost to orbit RBCC (HC-HC/H-H). This vehicle has a lower empty weight than the TSTO rockets and a wetted area comparable to the hydrogen TSTO rocket. Empty weight is considered a good figure of merit for the total cost of procuring a vehicle and one of the main figures of merit for maintaining and operating a vehicle. The growth rate of this vehicle is relatively low and comparable to that of TSTO rockets. The downside of this vehicle is that it uses three different types of propellants and the actual performance of a tri-propellant DMSJ is still uncertain.

3. The vehicle with the lowest wetted area is a tie between the HC-HC-H and all-hydrocarbon (HC-HC-HC) SSTO RBCC RLVs. Between these two vehicles, the all-hydrocarbon RLV is the better choice. This vehicle needs only two propellants, LOX and hydrocarbon fuel (such as RP-1). No cryogenic liquid hydrogen is used on this vehicle. This offers huge benefits for using a vehicle like this for military applications due to the lack of operationally obtrusive liquid hydrogen. Compared with TSTO rockets, the hydrocarbon SSTO RBCC has only a slightly higher empty mass. This vehicle is the best overall SSTO RLV. It has the smallest wetted area, one of the smallest empty masses, and does not use any liquid hydrogen. The only drawback of this vehicle is the uncertainty associated with RBCC vehicle technology.

5.3 Recommendations for Further Research

1. Airbreathing SSTO RLVs outperformed SSTO rocket systems in all figures of merit considered in this study. Additionally, the hydrocarbon fuel DMSJ showed clear mass and wetted area savings for airbreathing SSTO RLVs. Further study into RBCCs that use JP-7, methane and ethane could find an ideal hydrocarbon to use on a SSTO RLV. Besides the current problems getting it to burn in a scramjet, methane currently looks like a possible way to increase the I_{sp} of hydrocarbon fuel scramjets and increase the maximum velocity in which they can operate. The varying I_{sp}, densities and thermal properties of these different hydrocarbon fuels could lead to a vehicle with better mass and wetted area characteristics than the ones presented in this study.

2. There is still a great amount of uncertainty in scramjet technology. The only vehicle to ever use this form of propulsion is NASA's X-43. Methods for tank

construction, tank shape, tank placement, and payload integration are not well known. Further study into the internal layout of RBCC vehicles will greatly reduce the uncertainty of what these vehicles will actually look like when built. It is possible that the conservative assumptions in this study underestimated the packing efficiency of RBCC vehicles. By quantifying the methods for building RBCC vehicles, the uncertainty involved in studies like this one can be reduced.

3. A fully SSTO system is still at least fifteen to twenty years away. The logical next step on the way to single-stage is to use a current first-stage vehicle, such as an Aries III booster, in conjunction with a RBCC upper-stage. This upper-stage can be a scaled down version of a SSTO-capable design. Developing, testing and implementing a system like this would provide a great deal of data and experience on vehicles that can eventually be scaled up to single-stage. Proving the technology on a moderate-risk system will give policy makers the confidence they need to support and fund a SSTO project.

5.4 Summary

This study showed that an all-hydrocarbon, single-stage-to-orbit, reusable launch vehicle is not only a viable design, it is one of the best performing single-stage-to-orbit designs analyzed in this study. Single-stage rockets are too massive, require a great deal of thermal protection and are highly mass sensitive. Additionally, some of the airbreathing single-stage vehicles performed at the same level if not better than two-stage rockets. A great deal of research should be dedicated to hydrocarbon scramjet technology including determining the ideal fuel and methods for internal vehicle configuration. Using only hydrocarbons for fuel allows the vehicle to be used in military

applications requiring reusable, reliable and responsive access to space. Single-stage systems can offer the military reduced maintenance costs, simplified logistics, and enhanced reliability over current two-stage systems. These benefits may finally enable a significant reduction in the launch costs that inhibit the full use of space by government, military and civilian interests. While single-stage-to-orbit systems may still be decades away, their potential for improved space access should promote research into their development.

Appendix A. RDP Vehicle Shape

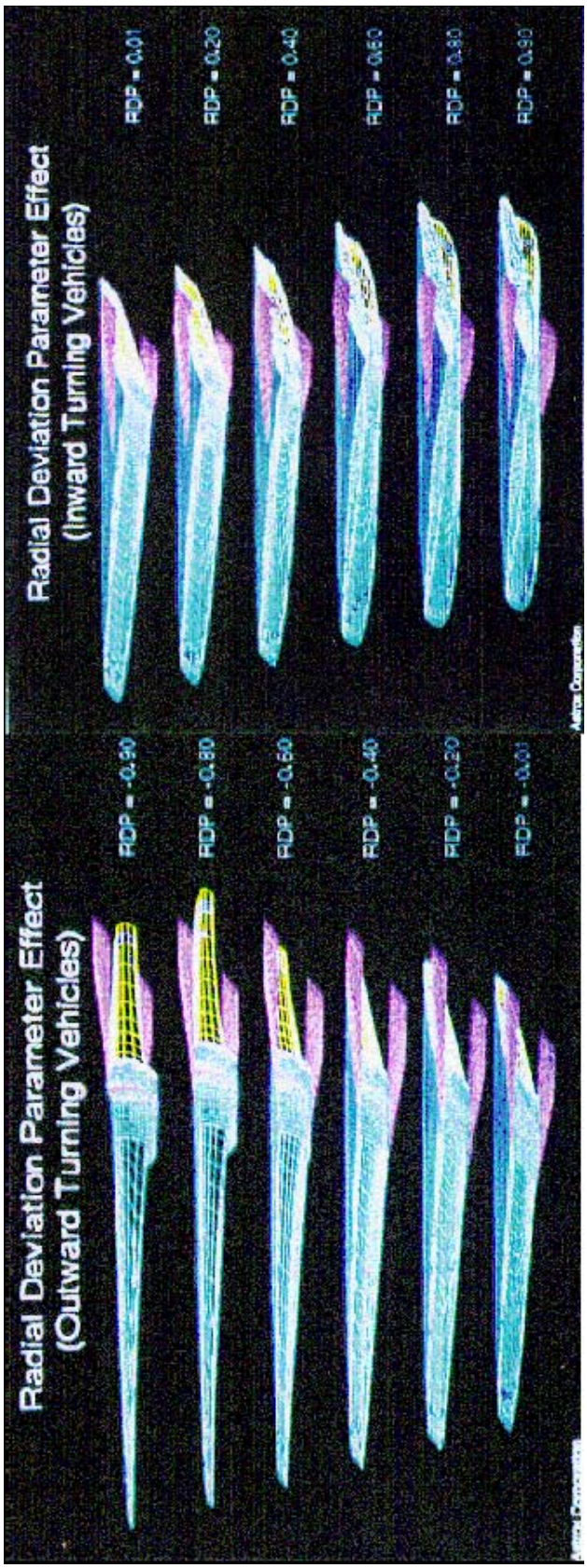

Figure 25. Radial Deviation Parameter (RDP) [16]

Appendix B. Airbreathing Engine Performance Data

Table 7. AFRL HyTech DMSJ Engine Performance Data [11]

Flight Path Angle = 0 deg			
Mach Number	Q (psf)	Thrust Coefficient	ISP (sec)
3.5	0	0	0
	250	0	0
	500	0	0
	1000	0	0
	2000	0	0
3.75	0	0	0
	250	0.546	1310.13
	500	0.728	1746.84
	1000	0.741	1759.93
	2000	0.745	1765.23
4.0	0	0	0
	250	0.632	1212.62
	500	0.843	1616.82
	1000	0.817	1621.24
	2000	0.822	1628.02
4.5	0	0	0
	250	0.586	1222.44
	500	0.782	1629.92
	1000	0.794	1639.12
	2000	0.805	1645.86
5.0	0	0	0
	250	0.666	1051.40
	500	0.888	1401.87
	1000	0.901	1408.23
	2000	0.909	1412.73
6.0	0	0	0
	250	0.419	701.00
	500	0.559	934.66
	1000	0.578	956.39
	2000	0.595	975.34
7.0	0	0	0
	250	0.346	605.15
	500	0.461	806.87
	1000	0.489	838.25
	2000	0.506	859.19
8.0	0	0	0
	250	0.284	532.38
	500	0.379	709.84
	1000	0.409	747.77
	2000	0.427	771.15
8.25	0	0	0
	250	0.270	514.30
	500	0.360	685.73
	1000	0.390	724.26
	2000	0.407	747.43

Flight Path Angle = 4 deg			
Mach Number	Q (psf)	Thrust Coefficient	ISP (sec)
3.5	0	0	0
	250	0	0
	500	0	0
	1000	0	0
	2000	0	0
3.75	0	0	0
	250	0.674	1344.75
	500	0.899	1793.00
	1000	0.914	1804.57
	2000	0.914	1800.45
4.0	0	0	0
	250	0.744	1218.96
	500	0.992	1625.28
	1000	1.014	1643.38
	2000	1.020	1648.68
4.5	0	0	0
	250	0.722	1225.07
	500	0.962	1633.43
	1000	0.977	1642.76
	2000	0.990	1649.38
5.0	0	0	0
	250	0.832	1050.79
	500	1.109	1401.05
	1000	1.127	1405.80
	2000	1.144	1409.60
6.0	0	0	0
	250	0.545	709.48
	500	0.727	945.97
	1000	0.751	964.88
	2000	0.772	981.51
7.0	0	0	0
	250	0.460	616.26
	500	0.613	821.68
	1000	0.649	849.72
	2000	0.671	868.22
8.0	0	0	0
	250	0.401	545.00
	500	0.534	726.66
	1000	0.573	760.93
	2000	0.597	782.85
8.25	0	0	0
	250	0.385	525.84
	500	0.513	701.12
	1000	0.553	736.59
	2000	0.577	758.03

Appendix C. Rocket Engine Specific Impulse

Table 8. Rocket Engine Specific Impulse

Alt (ft)	Alt (m)	SSME	RD-180	2T	2S	RD-701
0	0	401.1	313.8	369.6	352.0	330.0
10,500	3,200	411.9	319.3	380.1	362.0	339.2
18,375	5,601	422.7	324.8	391.7	373.0	344.8
23,625	7,201	425.5	326.2	399.0	380.0	347.4
26,250	8,001	428.3	327.6	402.2	383.0	348.4
28,875	8,801	430.4	329.8	403.3	387.0	349.2
34,125	10,401	432.4	332.0	404.8	393.0	351.1
65,625	20,003	449.0	342.0	405.0	405.0	355.1
131,250	40,005	458.7	349.8	408.0	408.0	357.6
210,000	64,008	458.9	350.0	459.3	459.3	459.3
257,802	78,578	459.0	350.1	459.8	459.8	459.8
300,000	91,440	459.0	350.1	459.8	459.8	459.8

Appendix D. HySIDE Design Inputs

Rocket Inputs

SysEl: RMLSRocketSystem5Mod

Inputs:

FreeStream	
Alt	Not critical for rockets, these two values are used by
Mach	airbreathers to set the constant Q value to fly at.
Rocket	
RocketFuselage	
RadiusMax	These values change the fuselage radius, conical nose
LengthOgive	section length and cylindrical fuselage length. Vary
LengthCylinder	these to get the right volume ratio
Reentry:	True
Wing	
WingUpperSurf	
Reentry:	True
WingLowerSurf	
Reentry:	True
Origin	Varies (Dependent on Fuselage Length)
LaunchMachNo	Used for landing speed
LaunchCL	Used for landing lift coefficient
EngineCluster	
Engine1/2/3/4/5	
DesignAltitude	Set for midway along path
AreaRatio1/2	Varies
FuelNumber	6 for JP-7, 1 for H_2
RocketParams_EEunits	2 for RD-180, 1 for SSME, Custom for tri-propellants
TankStack	
K_Factor_Overall	1.300
StructuralWeightsFromVol	
K_Factor_Overall	1.250
StructuralWeightsFromWt	
MassOfTakeOffPropulsion	
TurbineCluster	
Turbine	
ThrustToWeightAtTakeoff	1.4
RocketEngine_ToverW_Inst	HC: 75.000, H: 68.50000
Turbine	False
Fixed Weights	
PayloadAndAccomodations	9071.85 kg
PayloadVolume	79.29 m^3
PropellantUsage	
TrajSegment1	
V_Lo	Sourced Input
V_Hi	Sourced Input
VelISPMap	Varies
TrappedUnusableFraction	Set to 0.005 if this segment is used, else 0.0
ReserveFraction	Set to 0.010 if this segment is used, else, 0.0

StartupTime		3.00
TrajSegment2		
TrappedUnusableFraction		0.0 (This segment not used for rockets)
ReserveFraction		0.0 (This segment not used for rockets)
StartupTime		0.0 (This segment not used for rockets
TrajSegment3		
VelISPMap		Varies
TrappedUnusableFraction		Set to 0.005 if this segment is used, else 0.0
ReserveFraction		Set to 0.010 if this segment is used, else, 0.0
StartupTime		0.00
V1		Beginning of Seg1
V2		End of Seg1, Beginning of Seg2
V3		End of Seg2, Beginning of Seg3
V4		End of Seg3, Beginning of Seg4
PropTypeDetails:	HC:	Traj1: Fuel 2 (RP-1)/Oxidizer 1 (LOX) MR: 2.580
		Traj2: Fuel 1 (LH_2)
		Traj3: Fuel 1 (LH_2)/Oxidizer 1 (LOX) MR: 5.900
	H:	Traj1: Fuel 1 (LH_2)/Oxidizer 1 (LOX) MR: 5.900
		Traj2: Fuel 1 (LH_2)
		Traj3: Fuel 1 (LH_2)/Oxidizer 1 (LOX) MR: 5.900
Trajectory		
VelAltMap		
RocketDrag		Used if this stage is a rocket
RocketDragNextStage		Not used for SSTO)
WingDrag		Always used
FuselageDragNextStage		Not used for SSTO
ExtModDrag		Not uses
TrajStageName		stFirstStage
ThirdSegInitialHeight		000000.00
HeightFinal		303805.77
VelAltMapSeg1		Custom
VelAltMapSeg3		Custom
FuelStoichMassRatio		HC / H: 0.0288000
OrbitInclination		Change if a inclination change is desired
ExtModUsed		Change if external pod is used
WingUsed		True
PackingEfficiency		Booster: 0.90000
ThrustToWeightAtTakeoff		1.4

RBCC Inputs

SysEl: TSSTOSys2D2FIEqVTHL

Inputs:

FreeStream		
	Alt	Not critical for rockets, these two values are used by
	Mach	airbreathers to set the constant Q value to fly at.
HADOVehicleBasic		
	Inlet	
	InletGeom	
	InletMirrorGeom	
	RDP	0.99 for inward-turning, 0.01 for 2-D
	LH	Width/height ratio
	VehCapArea	Varies (Use this to size the vehicle)
	Comb	
	CombFlag	1
	FuelNumber	7 for JP-7 (Endo), 1 for LH2
	FuelTempMax	833 for Hydrogen, about 650 for Hydrocarbon
	Wing	
	Origin	Use this to move the wing around
	WingStrWtPerUnitArea	80.000
	LaunchMachNo	Landing speed
	LaunchCL	Landing lift coefficient
	VTail	
	PlanformScaleFactor	0.1000000
	TankStackAB	
	LH2Tank	
		K_Factor 1.4 for conformal tanks
	RP1Tank	
		K_Factor 1.4 for conformal tanks
	JP1Tank	
		K_Factor 1.4 for conformal tanks
	LOXTank	
		K_Factor 1.4 for conformal tanks
	StructuralWeightsFromVol	
	StructuralWeightsFromWt	
	MassOfTakeOffPropulsion	
	TurbineCluster	
	Turbine	
	TurbineGeom	
	TurbineGeomMirror	
	MMax	2.50
	ByPassRatio	0.950
	VolInstK_Factor	Set these to get good T/W
	WtInstK_Factor	installed value in outputs
	Afterburning	True
	Origin	Use this to move the single turbine
	NumberOfTurbines	Vary this for more turbines
	ThrustToWeightAtTakeoff	1.4
	RocketEngine_ToverW_Inst	HC: 80.00, LH2: 73.50
	TurbineEngine_ToverW_Inst	8.0000
	Turbine	False
	FlybackPropulsion	
	Engine1	
	Engine2	

TurbineToverW		3.000
AvgEISP		4500.00000
CruiseVel		Varies
Range		Varies
L_over_D		Varies
HeatLoopType		Use PhiTempLoop if FuelTempReached (in ouputs) exceeds FuelTempMax specified
GlobalPointLink		Use this to move vehicle around in viewer
Fixed Weights		
PayloadAndAccomodations		9071.85 kg
PayloadVolume		79.29 m^3
PropellantUsage		
TrajSegment1		
V_Lo		Sourced Input
V_Hi		Sourced Input
VelISPMap		LHC Rocket or LH2 Rocket, or Turbine
TrappedUnusableFraction		0.005
ReserveFraction		0.010
StartupTime		3.00
TrajSegment2		
V_Lo		Sourced Input
V_Hi		Sourced Input
VelISPMap		HC Ram-Scram or LH2 Ram-Scram New
VBegin		HC: 8000, H: 12000 (Temp at which fuel dump begins for cooling)
TrappedUnusableFraction		0.005
ReserveFraction		0.010
TrajSegment3		
VelISPMap		LHC Rocket or LH2 Rocket
TrappedUnusableFraction		0.005
ReserveFraction		0.010
StartupTime		0.00
V1		Beginning of Seg1
V2		End of Seg1, Beginning of Seg2
V3		End of Seg2, Beginning of Seg3
V4		End of Seg3, Beginning of Seg4
PropTypeDetails:	RBCC HC:	Traj1: Fuel 2 (RP1)/Oxidizer 1 (LOX) MR: 2.580 Traj2: Fuel 3 (JP1) Traj3: Fuel 1 (LH2)/Oxidizer 1 (LOX) MR: 2.580
	RBCC H:	Traj1: Fuel 2 (LH2)/Oxidizer 1 (LOX) MR: 5.900 Traj2: Fuel 3 (LH2) Traj3: Fuel 1 (LH2)/Oxidizer 1 (LOX) MR: 5.900
Trajectory		
RocketDrag		(Not used)
FuselageDrag		(Always used)
WingDrag		(Always used)
FuselageDragNextStage		(Not used on SSTO)
HeightInitial		0.000000 (ft)
ThirdSegHeightInitial		86000
HeightFinal		303805 (ft)
VelAltMapSeg1		RMLS Vertical Rocket @ 7000
VelAltMapSeg3		Horizontal Rocket
FuelStoichRatioSeg1Turbine		0.0673000
FuelStoichRatioSeg2RamScram		HC: 0.067300 LH2: 0.0291000
Turbine		False
UseFuselageDrag		True

UseFuselageDragNextStage	False
UseRocketDragNextStage	False
PackingEfficiency	0.85
GrossWeightNextStage	0.0000
VolumeNextStage	0.0000

Table 9. Full RLV HySIDE Outputs

Vehicle	GTOW (kg)	GTOW (lbs)	Empty Weight (kg)	Empty Weight (lbs)	Empty Mass Fraction	Payload Mass Fraction	Propellant Mass Fraction	Wetted Area (m^2)	Wetted Area (ft^2)	Length (m)	Length (ft)	Time of Flight (sec)	Time of Flight (min)
TSTO Rkt H	567,089	1,250,204	99,540	219,446	17.55%	1.60%	80.85%	2,566	27,624	37.69	123.62	262.5	4.4
TSTO Rkt HC	661,834	1,459,080	86,822	191,408	13.12%	1.37%	85.51%	1,814	19,527	27.53	90.30	287.3	4.8
SSTO Rkt H	1,320,538	2,911,258	174,387	384,455	13.21%	0.69%	86.10%	3,989	42,936	68.53	224.78	392.1	6.5
SSTO Rkt HC	2,709,250	5,972,812	202,748	446,978	7.48%	0.30%	92.22%	3,922	42,214	66.14	216.94	412.4	6.9
SSTO Rkt HC/H 2T	1,312,137	2,892,737	160,677	354,228	12.27%	0.69%	87.04%	3,418	36,787	66.18	217.07	353.9	5.9
SSTO Rkt HC/H 2S	1,247,459	2,750,148	152,276	335,707	12.21%	0.73%	87.06%	3,278	35,283	63.64	208.74	353.9	5.9
SSTO Rkt HC/H 1S	1,102,611	2,430,816	120,640	265,962	10.94%	0.82%	88.24%	2,948	31,734	58.60	192.20	338.5	5.6
TSTO Rkt H / RBCC H	265,027	584,278	72,366	159,539	27.31%	3.42%	69.27%	2,102	22,626	50.62	166.03	975.2	16.3
TSTO Rkt HC / RBCC H	286,723	632,109	61,431	135,430	22.57%	3.33%	74.10%	1,717	18,483	39.11	128.28	944.2	15.7
TSTO Rkt HC / RBCC HC	343,598	757,497	46,036	101,492	13.40%	2.64%	83.96%	1,183	12,736	30.95	101.52	925.4	15.4
SSTO RBCC H-H-H	571,436	1,259,787	137,288	302,666	24.03%	1.59%	74.38%	3,182	34,254	85.60	280.77	1,636.4	27.3
SSTO RBCC HC-H-H	481,360	1,061,206	102,673	226,353	21.02%	1.86%	77.12%	2,459	26,472	75.58	247.90	1,584.3	26.4
SSTO RBCC H-H-HC	*no covergance*												
SSTO RBCC HC-H-HC	1,193,883	2,632,034	180,068	396,978	15.08%	0.76%	84.16%	3,345	36,005	86.18	282.67	1,475.4	24.6
SSTO RBCC HC-HC/H-H	600,448	1,323,748	67,396	148,581	11.22%	1.51%	87.26%	2,337	25,154	71.10	233.21	1,237.5	20.6
SSTO RBCC HC-HC-H	555,971	1,225,693	84,784	186,914	15.03%	1.61%	83.36%	1,847	19,878	63.65	208.77	781.3	13.0
SSTO RBCC HC-HC-HC	943,285	2,079,566	107,776	237,602	11.25%	0.95%	87.80%	1,853	19,944	62.45	204.84	1,305.2	21.8

Appendix F. Vehicle Size Comparison

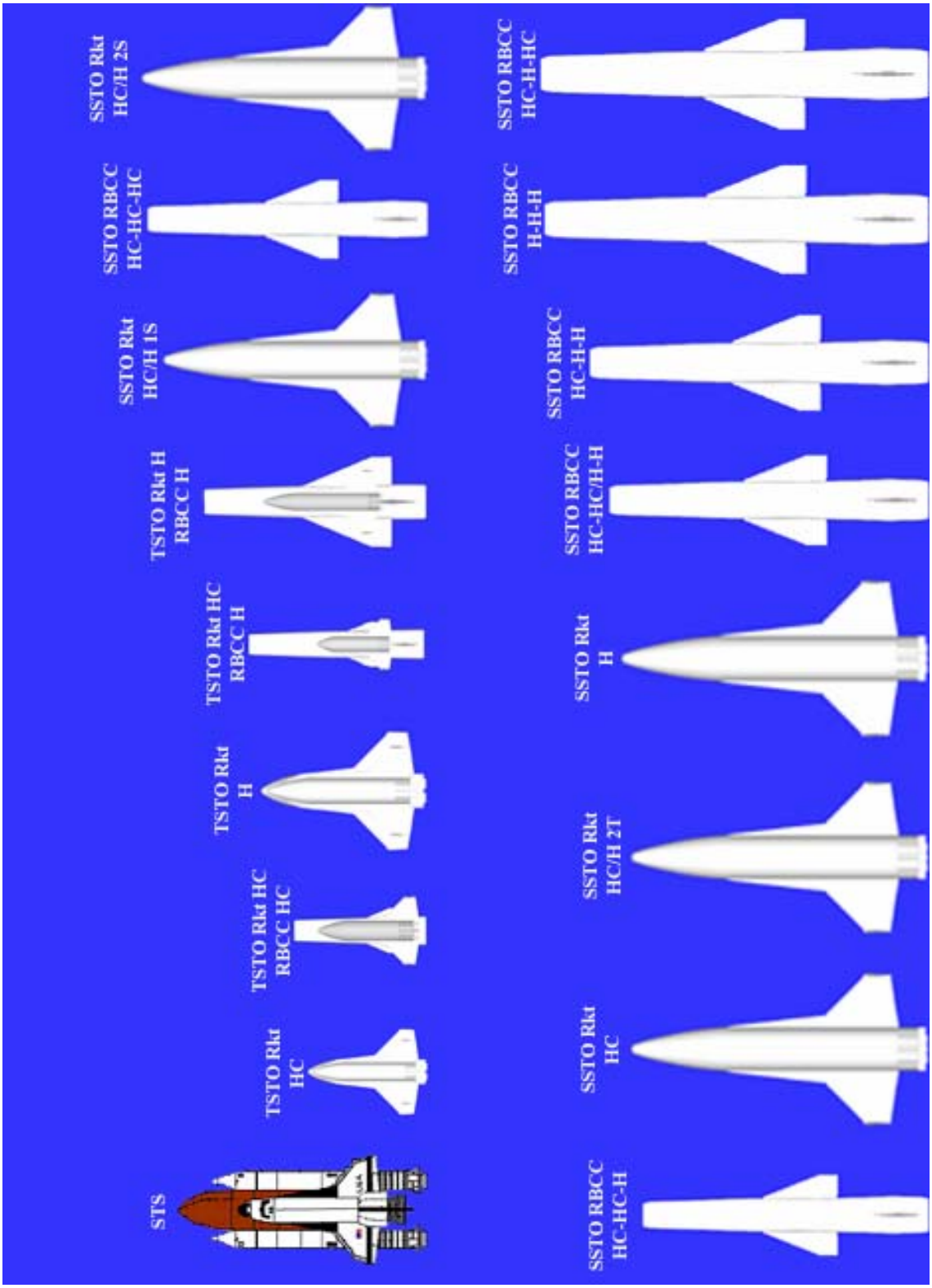

Figure 26. RLV Size Chart

Bibliography

1. Baurle, R. A. and D. R. Eklund. “Analysis of Dual-Mode Hydrocarbon Scramjet Operation at Mach 4 – 6.5”. AIAA 2001-3299, 37th AIAA/ASME/SAE/ASEE Joint Propulsion Conference and Exhibit, Salt Lake City UT, July 2001.

2. Bowcutt, Kevin, Mark Gonda, Steve Hollowell, and Ted Ralston. “Performance, Operational and Economic Drivers of Reusable Launch Vehicles.” AIAA 2002-3901, 38th AIAA/ASME/SAE/ASEE Joint Propulsion Conference and Exhibit, Indianapolis, IN, July 2002.

3. Brock, Marc A. *Performance Study of Two-Stage-to-Orbit Reusable Launch Vehicle Propulsion Alternatives.* MS Thesis, AFIT/GSS/ENY/04-M02. Graduate School of Engineering and Management, Air Force Institute of Technology (AU), Wright-Patterson AFB, OH, March 2004.

4. Caldwell, Richard J. *Weight Analysis of Two-Stage-to-Orbit Reusable Launch Vehicles for Military Applications.* MS Thesis, AFIT/GA/ENY/05-M02. Graduate School of Engineering and Management, Air Force Institute of Technology (AU), Wright-Patterson AFB, OH, March 2005.

5. Dissel, Adam F., Ajay P. Kothari, V. Raghavan, and Mark J. Lewis. “Comparison of HTHL and VTHL Air-Breathing and Rocket Systems for Access to Space.” AIAA 2004-3988, 40th AIAA/ASME/SAE/ASEE Joint Propulsion Conference and Exhibit, Fort Lauderdale, FL, 11-14 July 2004.

6. Dissel, Adam F., Ajay P. Kothari, and Mark J. Lewis. “Weight Growth Study of Reusable Launch Vehicle Systems.” AIAA 2005-4369, 41st AIAA/ASME/SAE/ASEE Joint Propulsion Conference and Exhibit, Tucson, AZ, 10-13 July 2005.

7. Dissel, Adam F. *Comparative System Analysis of Reusable Rocket and Air-breathing Launch Vehicles*. MS Thesis. Department of Aerospace Engineering, University of Maryland, College Park, MD, August 2005.

8. Dornheim, Michael A. “NASA's X-43A Hyper-X Reaches Mach 10 in Flight Test”. *Aviation Week & Space Technology*, http://www.aviationnow.com/avnow/, 23 November 2004.

9. Earp, Ted. “Advanced Air-Breathing Propulsion”. Presented to the Air Force Research Laboratory, Wright-Patterson AFB OH, 11 March 2003.

10. Gstattenbauer, Greg. *Cost Analysis of Launch Vehicles*. MS Thesis. AFIT/GAE/ENY/06-10. Graduate School of Engineering and Management, Air Force Institute of Technology (AU), Wright-Patterson AFB, OH, March 2006.

11. Hank, Joseph M. *Comparative Analysis of Two-Stage-To-Orbit Rocket and Airbreathing Reusable Launch Vehicles for Military Applications.* MS Thesis, AFIT/GAE/ENY/06-M12. Graduate School of Engineering and Management, Air Force Institute of Technology (AU), Wright-Patterson AFB, OH, March 2006.

12. Hill, Philip, and Carl Peterson. *Mechanics and Thermodynamics of Propulsion* (2nd Edition). New York: Addison-Wesley Publishing Company, 1992.

13. Humble, Ronald W., Gary N. Henry, and Wiley J. Larson. *Space Propulsion Analysis and Design* (Revised). New York: McGraw-Hill Publishing Company, 1995.

14. Hypersonic System Integrated Design Environment (HySIDE). Version 2.11, created using SIDE2000, version 4.0, CD-ROM. Computer Software. Astrox Corporation, College Park, MD, 2004.

15. Isakowitz, Steven J., Joshua Hopkins, and Joseph P. Hopkins, Jr. *International Reference Guide to Space Launch Systems* (4th Edition). Reston, VA: American Institute of Aeronautics and Astronautics, 2004.

16. Kothari, Ajay P., Christopher Tarpley, T.A. McLaughlin, Suresh Babu, and John W. Livingston. "Hypersonic Vehicle Design Using Inward Turning Flowfields." AIAA 96-2552, 32nd AIAA/ASME/SAE/ASME Joint Propulsion Conference, Lake Buena Vista, FL, 1-3 July 1996.

17. Lewis, Mark J. "Significance of Fuel Selection for Hypersonic Vehicle Range." *Journal of Propulsion and Power*, Vol. 17, No.6: 1214-1221 (November-December 2001).

18. Livingston, John W. "Comparative Analysis of Rocket and Air-breathing Launch Vehicles." AIAA-2004-5948. Space 2004 Conference and Exhibit, San Diego, CA, 28-30 September 2004.

19. Lyon, Jeffery A. "Abort Performance of a Winged-Body Single-Stage to Orbit Vehicle." NASA-CR-4690. Langley Research Center, National Aeronautics and Space Administration, 1995.

20. Powell, O. A., J. T. Edwards, R. B. Norris, K. E. Numbers, and J. A. Pearce. "Development of Hydrocarbon-Fueled Scramjet Engines: The Hypersonic Technology (HyTech) Program." *Journal of Propulsion and Power*, Vol. 17, No.6: 1170-1176 (November-December 2001).

21. Raymer, Daniel P. *Aircaft Design: A Conceptual Approach* (6th Printing). Reston, VA: American Institute of Aeronautics and Astronautics, 1999.

22. Rooney, Brendan D., and Alicia Hartong. “A Discrete-Event Simulation of Turnaround Time and Manpower of Military RLVs.” AIAA 2004-6111, Space 2004 Conference, San Diego, CA, September 28-30, 2004.

23. Snyder, Lynn E., Daric W. Escher, Rich L. DeFrancesco, Jose L. Gutierrez, and David L. Buckwalter. “Turbine Based Combined Cycle (TBCC) Subsystem Integration.” AIAA 2004-3649, 40th AIAA/ASME/SAE/ASEE Joint Propulsion Conference and Exhibit, Fort Lauderdale, FL, 11-14 July 2004.

24. Spires, David N. *Beyond Horizons: A Half Century of Air Force Space Leadership* (Revised Edition). Washington DC: U.S. Government Printing Office, 1998.

25. Whitehead, John C. “Single sate to orbit mass budgets derived from propellant density and specific impulse.” AIAA 1996-3108, 32nd AIAA/ASME/SAE/ASEE Joint Propulsion Conference and Exhibit, Lake Buena Vista, FL, 1-3 July 1996.

26. World Wide Web. http://neurolab.jsc.nasa.gov/answ_craft.htm

27. World Wide Web. http://nix.larc.nasa.gov/

28. World Wide Web. http://www.affordablespaceflight.com/nasa2.html

29. World Wide Web. http://www.aircraftenginedesign.com/custom.html4.html

30. World Wide Web. http://www.astronautix.com/

31. World Wide Web. http://www.daviddarling.info/encyclopedia/D/Dyna-Soar.html

32. World Wide Web. http://www.fas.org/spp/guide/usa/launch/x-43.htm

33. World Wide Web. http://www.globalsecurity.org/org/news/2003/030407-nasa01.htm

34. World Wide Web. http://www.howstuffworks.com/rocket.htm

35. World Wide Web. http://www.nasa.gov/mission_pages/exploration/multimedia

36. World Wide Web. http://www.nasa.gov/missions/research/x43-main.html

Vita

ENS Benjamin S. Orloff's comes from the small town of Issaquah, WA near Seattle. An Eagle Scout, he graduated from Issaquah High School in 2001 and accepted an appointment to the United States Naval Academy in Annapolis, MD. Upon graduating with honors in May of 2005, he received a commission as a naval officer and a Bachelor of Science degree in Aerospace Engineering with an emphasis is Astronautics. His first assignment was to the Air Force Institute of Technology at Wright-Patterson Air Force Base in Dayton, Oh as a part of the Navy's Immediate Graduate Education Program.

Upon graduation, he will be assigned to Training Air Wing Five and commence naval aviation training at Naval Air Station Pensacola in Florida. He is currently engaged and looks forward to be married in early 2007.

REPORT DOCUMENTATION PAGE

Form Approved
OMB No. 074-0188

1. REPORT DATE *(DD-MM-YYYY)*	2. REPORT TYPE	3. DATES COVERED *(From – To)*
13 JUN 06	Master's Thesis	July 2005 – June 2006

4. TITLE AND SUBTITLE

A Comparative Analysis of Single-Stage-to-Orbit Rocket and Airbreathing Vehicles

5a. CONTRACT NUMBER

5b. GRANT NUMBER

5c. PROGRAM ELEMENT NUMBER

6. AUTHOR(S)

Orloff, Benjamin S., Ensign, USN

5d. PROJECT NUMBER

5e. TASK NUMBER

5f. WORK UNIT NUMBER

7. PERFORMING ORGANIZATION NAMES(S) AND ADDRESS(S)

Air Force Institute of Technology
Graduate School of Engineering and Management (AFIT/EN)
2950 Hobson Way, Building 640
WPAFB OH 45433-8865

8. PERFORMING ORGANIZATION REPORT NUMBER

AFIT/GAE/ENY/06-J13

9. SPONSORING/MONITORING AGENCY NAME(S) AND ADDRESS(ES)

Dr. John Livingston
ASC / ENMD
1970 Monahan Way, Building 11a
WPAFB OH 45433 DSN: 785-3334

10. SPONSOR/MONITOR'S ACRONYM(S)

11. SPONSOR/MONITOR'S REPORT NUMBER(S)

12. DISTRIBUTION/AVAILABILITY STATEMENT

APPROVED FOR PUBLIC RELEASE; DISTRIBUTION UNLIMITED.

13. SUPPLEMENTARY NOTES

14. ABSTRACT

This study compares and contrasts the performance of a variety of rocket and airbreathing, single-stage-to-orbit, reusable launch vehicles. Fuels considered include bi-propellant and tri-propellant combinations of hydrogen and hydrocarbon fuels. Astrox Corporation's HySIDE code was used to model the vehicles and predict their characteristics and performance. Vehicle empty mass, wetted area and growth rates were used as figures of merit to predict the procurement, operational and maintenance cost trends of a vehicle system as well as the system's practicality. Results were compared to those of two-stage-to-orbit reusable launch systems using similar modeling methods. The study found that single-stage-to-orbit vehicles using scramjet airbreathing propulsion outperform rocket systems. Findings also demonstrate the benefits of using hydrocarbon fuel in the early phases of ascent to reduce the size and mass of launch vehicles. An all-hydrocarbon, airbreathing, single-stage-to-orbit vehicle was found to be a viable launch vehicle configuration and performed comparably to two-stage-to-orbit rocket systems.

15. SUBJECT TERMS

Singe-Stage-to-Orbit, Launch Vehicles, Hypersonic Vehicles, Rocket Propulsion, Space Propulsion, Space Launch, Propulsion Systems

16. SECURITY CLASSIFICATION OF:			17. LIMITATION OF ABSTRACT	18. NUMBER OF PAGES	19a. NAME OF RESPONSIBLE PERSON
REPORT	ABSTRACT	c. THIS PAGE			Dr. Milton Franke
U	U	U	UU	100	19b. TELEPHONE NUMBER *(Include area code)* (937) 255-6565, ext 4720 E-mail: Milton.Franke@afit.edu

Standard Form 298 (Rev: 8-98)
Prescribed by ANSI Std. Z39-18